Arabian Journal of Chemistry (2022) 15, 104115

King Saud University

Arabian Journal of Chemistry

www.ksu.edu.sa
www.sciencedirect.com

ORIGINAL ARTICLE

Vibration analysis of size dependent micro FML cylindrical shell reinforced by CNTs based on modified couple stress theory

Gang Zhao [a,*], Mostafa Hooman [b], Mahdireza Yarigarravesh [c], Mohammed Algarni [d], Maria Jade Catalan Opulencia [e], Fahad Alsaikhan [f], Abduladheem Turki Jalil [g], Abdullah Mohamed [h], Kareem M.AboRas [i], Md. Lutfor Rahman [j,*], Mohd Sani Sarjadi [j]

[a] *Architectural Engineering School, Qingdao Huanghai University, Qingdao, Shandong 266427, China*
[b] *Lyle School of Engineering, Southern Methodist University, Dallas, TX, USA*
[c] *Adjunct Faculty, Department of Civil Engineering, Sharif University of Technology, Tehran, Iran*
[d] *Mechanical Engineering Department, Faculty of Engineering, King Abdulaziz University, P.O. Box 344, Rabigh 21911, Saudi Arabia*
[e] *College of Business Administration, Ajman University, Ajman, United Arab Emirates*
[f] *College of Pharmacy, Prince Sattam Bin Abdulaziz University, Alkharj, Saudi Arabia*
[g] *Medical Laboratories Techniques Department, Al-Mustaqbal University College, Babylon, Hilla 51001, Iraq*
[h] *University Research Centre, Future University in Egypt, New Cairo 11745, Egypt*
[i] *Department of Electrical Power and Machines, Faculty of Engineering, Alexandria University, Alexandria, Egypt*
[j] *Faculty of Science and Natural Resources, Universiti Malaysia Sabah, 88400 Kota Kinabalu, Sabah, Malaysia*

Received 4 May 2022; accepted 7 July 2022
Available online 13 July 2022

KEYWORDS

Modified Stress Theory;
Vibration Analysis;
Agglomeration;
Micro cylindrical shell

Abstract In this manuscript, the sequel of agglomeration on the vibration of fiber metal laminated (FML) cylindrical shell in the micro phase using developed couple stress theory (MCST). Hamilton's principle has been carried out for deriving the non-classical equations of motion of size-dependent thin micro cylindrical shell on the basis of Love's first approximation theory. Mori-Tanaka and extended rule of mixture are utilized to estimate the mechanical attributes of carbon nanotubes (CNTs) and equivalent fiber, respectively. These four phases CNTs/fiber/polymer/metal laminated (CNTFPML) micro cylindrical shell is analyzed applying beam modal function model for

* Corresponding authors.
E-mail addresses: zhaog220221@163.com (G. Zhao), lotfor@ums.edu.my (Md. Lutfor Rahman).

Peer review under responsibility of King Saud University.

ELSEVIER Production and hosting by Elsevier

https://doi.org/10.1016/j.arabjc.2022.104115

several boundary limitations. Then, an investigation is performed to study the impacts of differing input parameters namely material length scale parameter, agglomeration, the distributions of agglomerated CNTs, the mass fraction of equivalent fiber and the volume fraction of CNTs on the frequency response of micro agglomerated CNTFPML cylindrical shell. The main output illustrated that the growth of frequencies is directly dependent to the increase of material length scale parameter for this agglomerated CNTFPML cylindrical shell so that through increasing the values of agglomeration parameters η and μ and material length scale parameter ℓ altogether, the frequencies of this cylindrical shell grow.

1. Introduction

Compared to metal, the application of composites has been grown in the previous decades due to of required to light weight and high strength structures and design ability to construct the structures with high stress tolerance in an arbitrary direction in modern engineering. More information about laminated composite structures and functionally graded materials (FGMs) can be observed with a deep consideration to the complementary references (Ghasemi and Mohandes, 2016; Mohammadimehr and Mohandes, 2015; Zhou et al., 2022; Chen et al., 2021; Chen et al., 2021; Mou and Bai, 2018; Baghlani et al., 2020; Khayat et al., 2020; Khayat et al., 2019; Khayat et al., 2017). Although composite materials have excellent strength, their fragile behavior under impact loading is an essential problem. This deficiency could be led to some critical problems namely crack, delamination and debonding, while ductile materials tolerate impact loading. So, using the combination of these two materials, which composite layers are bounded by aluminum metal face sheets to protect the composite materials, Fiber Metal Laminates (FMLs) were produced for more availability of the advantages of composites as well as metals in industries. FMLs have promoted their individual negative properties such as poor impact resistance of composites and poor fatigue strength of metals. Due to promoted mechanical properties of FMLs against composites and metals separately, their applications have been gradually increased in various industries such as fan blades in aeroengine, panels in military and civil aircrafts, solar panels in satellites. In addition, FMLs are applicable for complex environment under intense impact accidents namely hailstone, tool collisions, birds, and runway debris or under severe dynamic loading such as continuous drastic spinning imbalance loads. With increasing the usage of sandwich and FMLs in various industries, numerous investigations have been leaded to vibration of these structures (Mohandes et al., 2018; Ghasemi and Mohandes, 2019; Iriondo et al., 2015; Ghasemi and Mohandes, 2019; Khalili et al., 2010; Zhang et al., 2021; Liu et al., 2021) and the other structures (Wang et al., 2022; Ma et al., 2022; Tao et al., 2017). Tao et al. (Fu et al., 2014) obtained frequencies, mode shapes and deflection of FML Euler-Bernoulli beams with a single-open sided crack subjected to different boundary conditions. Some researchers (Fu and Shao, 2014) studied nonlinear geometrical dynamic of FML beam under thermal and mechanical loadings utilizing differential quadrature method. Nonlinear dynamic response of FML rectangular plate under thermal loading with interfacial damage was conducted by Fu and Shao (Ghasemi and Mohandes, 2020). Ghasemi and Mohandes (Mahmood et al., 2021) employed developed couple stress theory (MCST) to consider dynamic of micro FML cylindrical shell.

In the recent years, modern industries need materials which are applicable in different environmental circumstances such as variety of thermal, mechanical, and chemical properties as well as reasonable price. Carbon nanotubes (CNTs) are expected to have proper industrial potential due to their excellent thermal, mechanical and electrical properties such as great aspect ratio, high thermal, low density, high tensile strength, high elastic modulus, and electrical conductivities (Ghasemi and Mohandes, 2016; Ninh et al., 2021). They have attracted much attention and redundant applications in nano-engineering applications namely actuators, oil probes, nano reactors, chemical sensors, and support catalysts. Based on the mentioned benefits of CNTs in the field of structural mechanics, numerous studies have been conducted by researchers which are including both static and dynamic behaviors of nanocomposite structures (Ebrahimi and Seyfi, 2021; Miao et al., 2021; Moradi-Dastjerdi and Behdinan, 2021; Sheybani et al., 2021; Mohandes and Ghasemi, 2019; Ghasemi and Mohandes, 2019; Mohandes and Ghasemi, 2019; Mohammadimehr et al., 2016; Huang et al., 2021; Zerrouki et al., 2021; Arshid et al., 2021; Heidari et al., 2021; Bendenia et al., 2020; Pan et al., 2021; Behdinan et al., 2020; Qin et al., 2020; Qin et al., 2019; Liu et al., 2022; Sobhani and Masoodi, 2021; Sobhani et al., 2022; Sobhani et al., 2021; Rezaiee-Pajand et al., 2020; Nasution et al., 2022; Khayat et al., 2021; Khayat et al., 2021; Khayat et al., 2021; Khayat et al., 2021; Khayat et al., 2022; Mohammadimehr et al., 2018). Mohammadimehr et al. (Chakraborty et al., 2019) reached natural frequencies of cylindrical composite panel undergoing magneto-electro fields using first order shear deformation theory (FSDT). The composite panel was reinforced by different distributions of CNTs which were arranged in Poly-vinylidene fluoride matrix. Chakraborty et al. (SafarPour et al., 2019) analyzed nonlinear vibration and stability of pre-buckled and post-buckled laminated composite cylindrical panels reinforced by CNTs. They found out that the volume fraction of CNTs had a remarkable influence on vibration and post-buckling responses of this panel. SafarPour et al. (Zhu et al., 2012) considered the impact of critical voltage on vibration and buckling of rotating reinforced CNTs cylindrical shell. Free vibration and bending of reinforced composite plate based on FSDT were studied by Zhu et al. (Guo and Zhang, 2016). The outputs indicated that the natural frequencies and mode shapes were affected by different volume fraction of CNTs and width-to-thickness ratio. Guo and Zhang (Bousahla et al., 2020) considered nonlinear vibration of composite plates reinforced by CNTs undergoing combined in-plane and transverse excitations for simply supported boundary condition. Bousahla et al. (Shen and Xiang, 2012) focused on vibration and buckling of composite beam reinforced by CNTs.

Nonlinear vibration of composite shells with or without CNTs is one of the main matters of engineering and it has developed recently. In nonlinear vibration analysis of composite shells, it is significant to survey their frequencies and mode shapes, due to the structures of composite shell which often operate to dynamic loads in different situation. Shen and Xiang (Shen et al., 2017) proposed the vibration of reinforced composite cylinders under thermal loading using von-Karman assumption based on HSDT. Shen et a. (Li et al., 2020) considered the effects of graphene reinforced composites on the nonlinear vibration of laminated cylindrical shells undergoing thermal loading based on Reddy's third order shear deformation theory. Some researchers (Liu et al., 2021) promoted a new analytical model for prediction of strain parameters of composite shell reinforced by CNTs with partial constrained layer damping. They used Jones-Nelson nonlinear theory to analyze material properties as nonlinearity. Some researchers (Li et al., 2021) presented a novel method to optimize the nonlinear forced vibrations of FG shells fabricated applying piezoelectric materials in multi-physics fields undergoing electro-thermo-mechanical loadings. Both material and geometrical nonlinearities for vibration of fiber reinforced polymer composite cylindrical shells within thermal environment has been studied (Li et al., 2021). Some researchers (Li et al., 2021) considered nonlinear forced vibration of FGM sandwich cylindrical shells with porosities on an elastic substrate. The researchers (Ebrahimi and Beni, 2016) have been concentrated on the experimental and theoretical analyses of nonlinear vibration of fiber-reinforced composite cylindrical shells with bolted joint boundary limitations.

The material's stiffness and strength can be increased with decreasing the size scale that is named size effects. The classical continuum mechanics theory is unable to count the size effects in micro scale structures, while some higher order continuum theories have been used to specify the size effect. The strain gradient approach and couple stress theory (CST) are used for micro structures with a bit difference. The variable for describing curvature is introduced using strain and rotation for strain gradient and couple stress theories, respectively. As a conclusion, it can be understood that the CST is a specific form of the strain gradient theory. Ebrahimi and Beni (Akgoz and Civalek, 2011) obtained natural frequencies of short piezoelectric cylindrical nanotube using shear deformable cylindrical theory according to consistent CST. Akgoz and Civalek (Akgoz and Civalek, 2016; Habibi et al., 2019) used strain gradient elasticity and MCST for buckling and bending analysis of micro beams. Habibi et al. (Zeighampour and Beni, 2014) applied MCST for nonlinear free vibration of magneto-electro-elastic Euler-Bernoulli nano beams under thermal loading. Zeighampour and Beni (Zeighampour and Beni, 2014) utilized strain gradient theory for developing cylindrical thin-shell model to analyze free vibration of CNTs subjected to simply-supported boundary condition. In the same study (Pashmforoush, 2020) they studied free vibration of thin conical shells utilizing MCST. Pashmforoush (Mehralian and Beni, 2018) considered low velocity impact response of composites reinforced by CNTs based on finite element model using Hashin's criterion and cohesive zone modeling. Mehralian and Beni (Soleimani and Beni, 2018) applied strain gradient theory for dynamic replies of bimorph FG piezoelectric cylindrical shell via FSDT. The natural frequencies of axisymmetric shell element using MCST were obtained by Soliemani and Beni (Zeighampour and Beni, 2017). Zeighampour and Beni (Sobhani et al., 2022) studied wave propagation of FG micro cylindrical shell reinforced by CNTs using strain gradient theory based on shear deformable shell theory.

Although CNTs have some efficiencies that promote electro-thermo-mechanical properties of structures and these benefits are existed when they uniformly dispersed in the matrix, they have a deficiency which is agglomeration. They tend to be agglomerated in a cluster because of their maximum aspect ratio (usually > 1000) and low bending stiffness because of small diameter and/or elastic modulus in the radial direction (Allahkarami and Nikkhah-Bahrami, 2017). Allahkarami and Nikkhah-bahrami (Ebrahimi et al., 2019) studied free vibration of CNTs reinforced micro curved Timoshenko beam with considering agglomeration factors using generalized differential quadrature method. Another article in this interest field was arranged by Ebrahimi et al. (Ebrahimi et al., 2019) dealing with the efficiency of agglomeration on the vibration of multi-scale hybrid plates reinforced by CNTs. Ebrahimi et al. (García-Macías and Castro-Triguero, 2018) could analytically solve the equations of motion for wave frequency and phase velocity of multi-scale hybrid CNTs reinforced beams with agglomeration effects. García-Macías and Castro-Triguero (Daghigh and Daghigh, 2019) presented the effects of waviness and agglomeration on vibration of CNTs reinforced skew plates. Daghigh and Daghigh (Afshari and Amirabadi, 2021) successfully probed free vibration of agglomerated composite plates reinforced by CNTs mounted on elastic foundation under thermal loading. Afshari and Amirabadi (Ghasemi et al., 2019) surveyed the effect of rotational speed on agglomerated CNTs reinforced truncated conical shells based on FSDT using a semi-analytical solution. The issue of vibration of FML CNTs reinforced cylindrical shell has been studied (Syah et al., 2021) with the consideration of agglomeration effects. Some researchers (Yang et al., 2002) highlighted the influences of rotation on the frequencies of FML rotating CNTs reinforced circular cylindrical shells with agglomerated nanoparticles.

Then, no literatures have been reported on the vibration response of agglomerated micro cylindrical shells specially CNTs/fiber/polymer/metal laminated (CNTFPML) micro cylindrical shell. It means the effect of agglomeration in micro phase of CNTFPML for vibration analysis has not been considered, yet. The vibration analysis of this material can be applied in aerospace industries because of proper properties of metal namely impact, damage tolerance and ductility plus the appropriate characteristics of the composites such as excellent fatigue resistance, stiffness to weight ratios, high strength and acceptable corrosion. In this investigation, the agglomeration effects on this micro cylindrical shell are studied on the basis of Love's first approximation theory. The structure is including four phases: CNTs, fiber, polymer matrix and metal layers which are attached together. The equations of motion for this CNTFPML micro cylindrical shell are obtained utilizing Hamilton's principle so that the size effect is considered in these equations using MCST. In addition, the frequencies of structure are calculated utilizing the beam modal function model that is semi-analytical model for considering different boundary conditions.

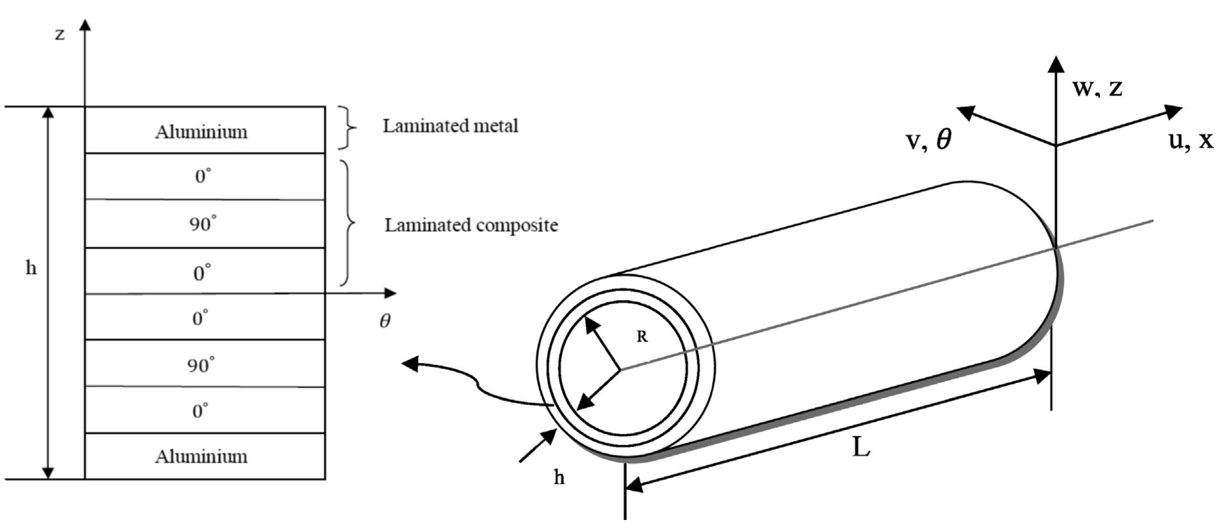

Fig. 1 CNTFPML micro cylindrical shell (Mahmood et al., 2021)

2. Formulation

In this section, the necessary equations related to dynamic analysis of CNTFPML micro cylindrical shell (Figure 1) with considering agglomeration relations are derived. As depicted in Fig. 1, the composite section of cylindrical shell has been considered cross-ply [Al/0°/90°/0°] so that the metal thickness is same as each layer of composites.

Also, in the following flowcharts 1, the steps for constructing the whole structure as well as the procedure of finding natural frequencies of the micro agglomerated CNTFPML structure are shown.

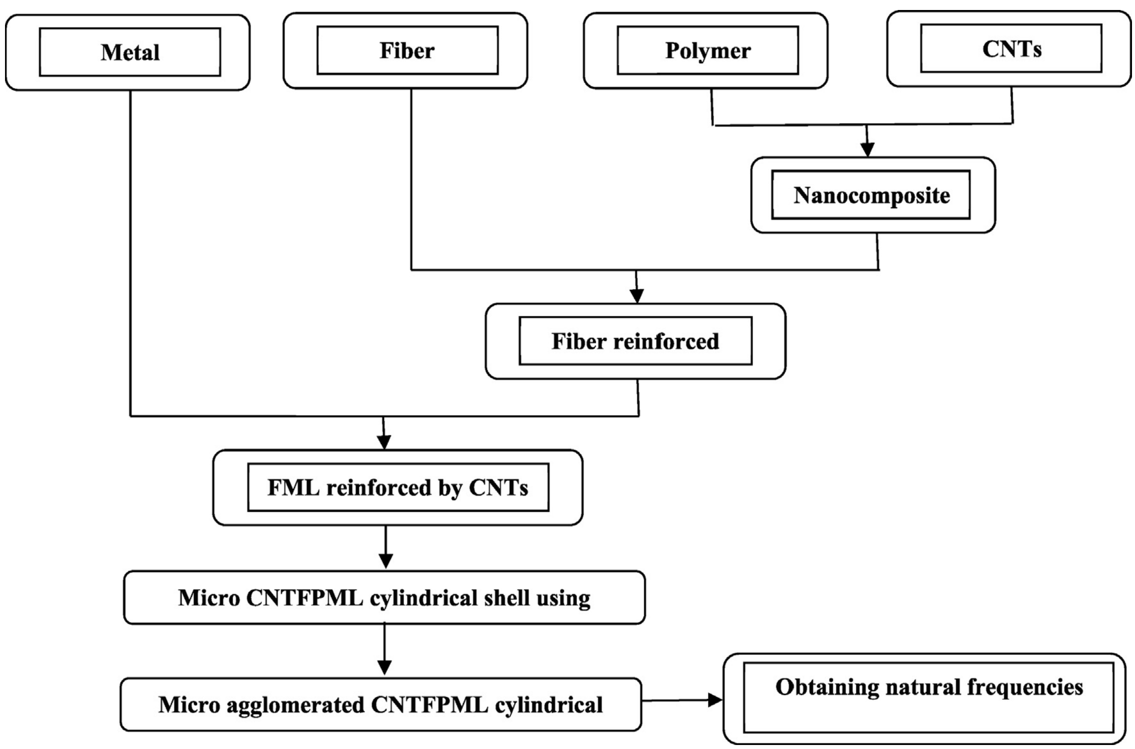

Flowchart 1. Steps for Obtaining natural frequencies of Micro agglomerated CNTFPML cylindrical shell.

2.1. Modified couple stress theory

Compared to classical CST which is involved only single scale parameter ℓ, the MCST defines the strain energy utilizing a function of both strain and curvature tensors which are including length scale parameter as well as Lame's constants (Hadjesfandiari and Dargush, 2018):

$$U = \frac{1}{2}\int_V (m_{ij}\chi_{ij} + \sigma_{ij}\varepsilon_{ij})dv \, (i,j = x,\, \theta,\, z) \tag{1}$$

$$\sigma_{ij} = 2\mu\varepsilon_{ij} + \lambda\varepsilon_{ii} \tag{2}$$

$$\varepsilon_{ij} = \frac{1}{2}\left(u_{i,j} + u_{j,i}\right) \tag{3}$$

$$m_{ij} = 2\mu\ell^2\chi_{ij} \tag{4}$$

$$\chi_{ij} = \frac{1}{2}\left(\nabla\varphi_i + (\nabla\varphi_i)^T\right) = \frac{1}{2}\left(\frac{\partial\varphi_i}{\partial x_j} + \frac{\partial\varphi_j}{\partial x_i}\right) \tag{5}$$

Deviatoric part of the symmetric couple stress tensor, strain tensor, stress tensor, and symmetric curvature tensor are shown using m_{ij}, ε_{ij}, σ_{ij}, , and χ_{ij}, respectively. Also, λ and μ are Lame's constants, and the material length scale parameter is indicated by ℓ which is estimated by means of experimental tests (Hadjesfandiari et al., 2016; Mohammad-Abadi and Daneshmehr, 2015). In addition, u is displacement and ϕ is the rotation vector relevant to the displacement which is described as (Lee and Kim, 1998):

$$\varphi_i = \frac{1}{2}(curl(u))_i \tag{6}$$

2.2. Love's first approximation theory

Due to the underlying hypothesis of Love's thin shell theory, the displacement field of micro circular cylindrical shell would be given as (Ma et al., 2008):

$$u_1(x,\, \theta,\, z,\, t) = -z\frac{\partial w(x,\, \theta,\, t)}{\partial x} + u(x,\, \theta,\, t) \tag{7}$$

$$u_2(x,\, \theta,\, z,\, t) = -\frac{z}{R}\left(\frac{\partial w(x,\, \theta,\, t)}{\partial x}\right) + v(x,\, \theta,\, t)$$

$$u_3(x,\, \theta,\, z,\, t) = w(x,\, \theta,\, t)$$

U(x.θ.t), V(x.θ. t) and W(x.θ. t) are the neutral plane displacements along through the coordinate directions x, θ and z. Besides, R is the radius of the shell. The nonzero strain components for micro shells relevant to displacements can be obtained as (Mohandes et al., 2018):

$$\varepsilon_{xx} = -z\frac{\partial^2 w}{\partial x^2} + \frac{\partial u}{\partial x} \tag{8}$$

$$\varepsilon_{\theta\theta} = -\frac{z}{R^2}\left(\frac{\partial^2 w}{\partial \theta^2} - \frac{\partial v}{\partial \theta}\right) + \frac{1}{R}\left(\frac{\partial v}{\partial \theta} + w\right)$$

$$\varepsilon_{x\theta} = \frac{\partial v}{\partial x} + \frac{1}{R}\frac{\partial u}{\partial \theta} - \frac{2z}{R}\left(\frac{\partial^2 w}{\partial x \partial \theta} - \frac{\partial v}{\partial x}\right)$$

The nonzero components of rotation vector and curvature tensor related to displacements are given like (Mahmood et al., 2021):

$$\varphi_x = \frac{1}{2}\left(\frac{\partial w}{\partial \theta} + \frac{1}{R}\frac{\partial w}{\partial \theta}\right) \tag{9}$$

$$\varphi_\theta = -\frac{\partial w}{\partial x}$$

$$\varphi_z = \frac{1}{2}\left(z\frac{\partial^2 w}{\partial x \partial \theta} + \frac{\partial v}{\partial x} - \frac{\partial u}{\partial \theta} - \frac{z}{R}\frac{\partial^2 w}{\partial x \partial \theta}\right)$$

$$\chi_{xx} = \frac{1}{2}\left(\frac{1}{R}\frac{\partial^2 w}{\partial x \partial \theta} + \frac{\partial^2 w}{\partial x \partial \theta}\right) \tag{10}$$

$$\chi_{\theta\theta} = -\frac{\partial^2 w}{\partial x \partial \theta}$$

$$\chi_{zz} = \frac{1}{2}\left(\frac{\partial^2 w}{\partial \theta \partial x} - \frac{1}{R}\frac{\partial^2 w}{\partial \theta \partial x}\right)$$

$$\chi_{x\theta} = \frac{1}{2}\left(\frac{1}{2}\left(\frac{\partial^2 w}{\partial \theta^2} + \frac{1}{R}\frac{\partial^2 w}{\partial \theta^2}\right) - \frac{\partial^2 w}{\partial x^2}\right)$$

$$\chi_{xz} = \frac{1}{4}\left(\frac{\partial^2 v}{\partial x^2} - \frac{\partial^2 u}{\partial x \partial \theta} - \frac{z}{R}\frac{\partial^3 w}{\partial x^2 \partial \theta} + z\frac{\partial^3 w}{\partial x^2 \partial \theta}\right)$$

$$\chi_{z\theta} = \frac{1}{4}\left(z\frac{\partial^3 w}{\partial x \partial \theta^2} + \frac{\partial^2 v}{\partial x \partial \theta} - \frac{z}{R}\frac{\partial^3 w}{\partial x \partial \theta^2} - \frac{\partial^2 u}{\partial \theta^2}\right)$$

3. Governing equations of motion

Hamilton's principle is applied to derive the governing equations of motion with boundary limitations for micro cylindrical shell as follows (Ma et al., 2008; Reddy, 2017; Beni et al., 2016):

$$\int_0^T \delta L dt = \int_0^T (\delta T - (\delta U - \delta W)dt = 0 \tag{11}$$

L represents Lagrangian function. Moreover, δT, δU and δW express virtual kinetic energy, virtual strain energy and virtual work.

In consideration of Eq. (1), virtual form of strain energy is calculated as (Mahmood et al., 2021):

$$\begin{aligned}\delta U &= \int_V (\sigma_{ij}\delta\varepsilon_{ij} + m_{ij}\delta\chi_{ij})dv \\ &= \int_V \begin{matrix}(\sigma_{xx}\delta\varepsilon_{xx} + \sigma_{\theta\theta}\delta\varepsilon_{\theta\theta} + m_{xx}\delta\chi_{xx} + m_{\theta\theta}\delta\chi_{\theta\theta} + 2m_{x\theta}\delta\chi_{x\theta} \\ +2m_{xz}\delta\chi_{xz} + 2m_{z\theta}\delta\chi_{z\theta})dv\end{matrix}\end{aligned} \tag{12}$$

The stress resultants N and M which are forces and moments (Reddy, 2004):

$$\{N_{\theta\theta}, N_{xx},\ N_{x\theta}\} = \int_{-h/2}^{h/2} \{\sigma_{\theta\theta},\ \sigma_{xx},\ \sigma_{x\theta}\}dz \tag{13}$$

$$\{M_{\theta\theta}, M_{xx},\ M_{x\theta}\} = \int_{-h/2}^{h/2} \{\sigma_{\theta\theta}, \sigma_{xx},\ \sigma_{x\theta}\}zdz$$

Y and P, which are couple moment and high order resultant of normal stress, are illustrated (Reddy, 2004):

$$\{Y_{xz},\ Y_{z\theta}\} = \int_{-h/2}^{h/2} \{m_{xz},\ m_{z\theta}\}zdz \tag{14}$$

$$\{P_{xx},\ P_{\theta\theta},\ P_{x\theta},\ P_{xz},\ P_{z\theta}\} = \int_{-h/2}^{h/2} \{m_{xx},\ m_{\theta\theta},\ m_{x\theta},\ m_{xz},\ m_{z\theta}\}dz$$

The kinetic energy and work done using external loading (in which q is zero in this study) are obtained as (Shi et al., 2004):

$$\begin{aligned}\delta T &= \int_0^L \int_A \rho\frac{\partial u_i}{\partial t}\delta\left(\frac{\partial u_i}{\partial t}\right)dAdx = \rho A\int_0^L \frac{\partial u}{\partial t}\delta\left(\frac{\partial u}{\partial t}\right)dx \\ &+ \rho A\int_0^L \frac{\partial v}{\partial t}\delta\left(\frac{\partial v}{\partial t}\right)dx + \rho A\int_0^L \frac{\partial w}{\partial t}\delta\left(\frac{\partial w}{\partial t}\right)dx\end{aligned} \tag{15}$$

$$\delta W = \int_0^L q\delta u_i dx \tag{16}$$

The stiffness coefficients for micro CNTFPML cylindrical shells can be described as (Mahmood et al., 2021):

$$A_{ij} = Q_{ij}^m h_m + \textstyle\sum_{k=1}^N Q_{ij}^k (h_k - h_{k-1}) \tag{17a}$$

$$B_{ij} = \frac{1}{2}\sum_{k=1}^N Q_{ij}^k (h_k^2 - h_{k-1}^2) \tag{17b}$$

$$D_{ij} = \frac{1}{12}Q_{ij}^m h_m^3 + \frac{1}{3}\sum_{k=1}^N Q_{ij}^k (h_k^3 - h_{k-1}^3) \tag{17c}$$

A_{ij}, B_{ij} and D_{ij} denote extensional, coupling and bending stiffnesses. In addition, the distances of the middle surface of the shell to outer and inner surfaces of the composite kth layer are shown as h_k and h_{k-1}. Here, Q_{ij}^k stand for the coefficients of transformed reduced stiffness for the kth layer of nanocomposites. Then, h_m and Q_{ij}^m are the thickness and decreased stiffness of the metal layer, respectively.

$$Q_{11} = \frac{E_{c,L}}{1 - \upsilon_L\upsilon_T}\ Q_{22} = \frac{E_{c,T}}{1 - \upsilon_L\upsilon_T}\ Q_{12} = \frac{\upsilon_T E_{c,L}}{1 - \upsilon_L\upsilon_T}\ Q_{66} = G_c \tag{18}$$

in which $E_{c\cdot L}$, $E_{c\cdot T}$ and G_c express longitudinal, transverse and shear modulus of the nanocomposite. In addition, effective Poisson's ratios are indicated as υ_L and υ_T. The elastic modulus and Poisson's ratios of CNTFPML circular cylindrical shell are described as:

$$E_{c,L} = E_{11,f}V_f + E_{11,new}^m V_{m,new}\ E_{c,T} = \frac{1}{\frac{V_f}{E_{22,f}} + \frac{V_{m,new}}{E_{22,new}^m}}\ G_c = \frac{1}{\frac{V_f}{G_f} + \frac{V_{m,new}}{G_{12,new}^m}}$$

$$\upsilon_L = \upsilon_f V_f + \upsilon_{m,new}V_{m,new}\ \upsilon_T = \upsilon_L \times \frac{E_{c,T}}{E_{c,L}} \tag{19}$$

where subscript f denotes the elastic modulus of fiber phase. Also, subscript new with superscript m and subscript m. new stand for matrix phase reinforced by the CNTs. Moreover, V specifies the volume fraction.

The equations of motion can be obtained using substitution Eqs. (12), (15) and (16) into Hamilton's principle. It is worth noticing that the equations of motion are obtained based on stress resultants, while they shall be according to displacements for better application. So, the stress resultants shall be rewritten based on changes in the curvature of the middle surface and middle surface strains at first. Since then, the equations of motion for micro CNTFPML cylindrical shell shall be calculated based on displacements by introducing the resulted stress resultants and Eq. (14) into Eq. (20) as given:

$$\begin{aligned}&A_{11}\frac{\partial^2 u}{\partial x^2}+\frac{1}{R}A_{12}\left(\frac{\partial^2 v}{\partial x\partial\theta}+\frac{\partial w}{\partial x}\right)-B_{11}\frac{\partial^3 w}{\partial x^3}\\&\quad+\frac{1}{R^2}B_{12}\left(-\frac{\partial^3 w}{\partial x\partial\theta^2}+\frac{\partial^2 v}{\partial x\partial\theta}\right)+\frac{1}{R}A_{66}\frac{\partial^2 v}{\partial x\partial\theta}+\frac{1}{R^2}A_{66}\frac{\partial^2 u}{\partial\theta^2}\\&\quad+\frac{2}{R^2}B_{66}\left(-\frac{\partial^3 w}{\partial x\partial\theta^2}+\frac{\partial^2 v}{\partial x\partial\theta}\right)\\&\quad+\frac{1}{4}\mu\ell^2 h\left(\frac{\partial^4 v}{\partial x^3\partial\theta}-\frac{\partial^4 u}{\partial x^2\partial\theta^2}+\frac{\partial^4 v}{\partial x\partial\theta^3}-\frac{\partial^4 u}{\partial\theta^4}\right)-\rho h\ddot{u}=0\end{aligned}\tag{20a}$$

$$\begin{aligned}&\frac{1}{R}A_{12}\frac{\partial^2 u}{\partial x\partial\theta}+A_{66}\frac{\partial^2 v}{\partial x^2}+\frac{1}{R}A_{66}\frac{\partial^2 u}{\partial x\partial\theta}+\frac{2}{R}B_{66}\left(\frac{\partial^2 v}{\partial x^2}-\frac{\partial^3 w}{\partial x^2\partial\theta}\right)\\&+\frac{1}{R^3}B_{22}\left(\frac{\partial^2 v}{\partial\theta^2}-\frac{\partial^3 w}{\partial\theta^3}\right)+\frac{1}{R^2}A_{22}\left(\frac{\partial^2 v}{\partial\theta^2}+\frac{\partial w}{\partial\theta}\right)\\&+\frac{1}{R^2}B_{66}\frac{\partial^2 u}{\partial x\partial\theta}-\frac{1}{R}B_{12}\frac{\partial^3 w}{\partial x^2\partial\theta}+\frac{1}{R}B_{66}\frac{\partial^2 v}{\partial x^2}\\&+\frac{1}{R^3}B_{22}\left(\frac{\partial w}{\partial\theta}+\frac{\partial^2 v}{\partial\theta^2}\right)+\frac{2}{R^2}D_{66}\left(\frac{\partial^2 v}{\partial x^2}-\frac{\partial^3 w}{\partial x^2\partial\theta}\right)\\&-\frac{1}{R^2}D_{12}\frac{\partial^3 w}{\partial x^2\partial\theta}+\frac{1}{R^2}B_{12}\frac{\partial^2 u}{\partial x\partial\theta}+\frac{1}{R^4}D_{22}\frac{\partial^2 v}{\partial\theta^2}-\frac{1}{R^4}D_{22}\frac{\partial^3 w}{\partial\theta^3}\\&-\frac{1}{4}\mu\ell^2 h\left(\frac{\partial^4 v}{\partial x^4}-\frac{\partial^4 u}{\partial x^3\partial\theta}+\frac{\partial^4 v}{\partial x^2\partial\theta^2}-\frac{\partial^4 u}{\partial x\partial\theta^3}\right)-\rho h\ddot{v}=0\end{aligned}\tag{20b}$$

$$\begin{aligned}&B_{11}\frac{\partial^3 u}{\partial x^3}-D_{11}\frac{\partial^4 w}{\partial x^4}+\frac{1}{R}B_{12}\left(\frac{\partial^2 w}{\partial x^2}+\frac{\partial^3 v}{\partial x^2\partial\theta}\right)\\&+\frac{2}{R}B_{66}\frac{\partial^3 v}{\partial x^2\partial\theta}+\frac{1}{R^2}D_{12}\left(\frac{\partial^3 v}{\partial x^2\partial\theta}-\frac{\partial^4 w}{\partial x^2\partial\theta^2}\right)\\&+\frac{4}{R^2}D_{66}\left(\frac{\partial^3 v}{\partial x^2\partial\theta}-\frac{\partial^4 w}{\partial x^2\partial\theta^2}\right)+\frac{2}{R^2}B_{66}\frac{\partial^3 u}{\partial x\partial\theta^2}\\&+\frac{1}{R^3}B_{22}\left(\frac{\partial^2 w}{\partial\theta^2}+\frac{\partial^3 v}{\partial\theta^3}\right)+\frac{1}{R^2}B_{12}\frac{\partial^3 u}{\partial x\partial\theta^2}\\&+\frac{1}{R^4}D_{22}\left(\frac{\partial^3 v}{\partial\theta^3}-\frac{\partial^4 w}{\partial\theta^4}\right)-\frac{1}{R^2}D_{12}\frac{\partial^4 w}{\partial x^2\partial\theta^2}+\frac{1}{R}B_{12}\frac{\partial^2 w}{\partial x^2}\\&-\frac{1}{R}A_{12}\frac{\partial u}{\partial x}-\frac{1}{R^2}A_{22}\left(\frac{\partial v}{\partial\theta}+w\right)+\frac{1}{R^3}B_{22}\left(\frac{\partial^2 w}{\partial\theta^2}-\frac{\partial v}{\partial\theta}\right)\\&-\frac{1}{2}\mu\ell^2 h\left(\frac{1}{2}\frac{\partial^4 w}{\partial\theta^4}+\frac{1}{R^2}\frac{\partial^4 w}{\partial\theta^2\partial x^2}+\frac{1}{2R}\frac{\partial^4 w}{\partial\theta^4}+\frac{2}{R}\frac{\partial^4 w}{\partial\theta^2\partial x^2}\right)\\&-\frac{1}{2R}\mu\ell^2 h\left(\frac{1}{2}\frac{\partial^4 w}{\partial\theta^4}-\frac{\partial^4 w}{\partial\theta^2\partial x^2}+\frac{1}{2R}\frac{\partial^4 w}{\partial\theta^4}\right)\\&+\mu\ell^2 h\left(\frac{3}{2}\frac{\partial^4 w}{\partial\theta^2\partial x^2}-\frac{\partial^4 w}{\partial x^4}+\frac{3}{2R}\frac{\partial^4 w}{\partial\theta^2\partial x^2}\right)\\&-\rho h\ddot{w}=0\end{aligned}\tag{20c}$$

4. Agglomeration

The agglomeration of CNTs would influence on the elastic attributes of CNTRCs that this effect can be focused using a micromechanical model, which has been presented here. The agglomeration causes some CNTs are appeared in the cluster (concentrated region) and the others are distributed within the matrix (Fig. 2a) (Dabbagh et al., 2020). So, there are some limited clusters including CNTs which are settled in the whole matrix as well as distributed CNTs outside the clusters. So, CNTs' concentration which creates the degradation of elastic properties would be different from the other regions.

Thus, the CNTs volume inside $V_r^{cluster}$ and outside V_r^m the cluster constitute the total volume of CNTs which is indicated by V_r (Hedayati and Sobhani Aragh, 2012):

$$V_r=V_r^{cluster}+V_r^m\tag{21}$$

Also, the total volume of representative volume element (RVE) V (Hedayati and Sobhani Aragh, 2012):

$$V=V_r+V_m\tag{22}$$

where V_m is the volume of matrix. Two agglomeration parameters are introduced to investigate agglomeration effects of CNTs in the following formulations (Hedayati and Sobhani Aragh, 2012):

$$\mu=\frac{V_{cluster}}{V}\ \eta=\frac{V_r^{cluster}}{V_r}\ \eta\geqslant 0\,,\ \mu\leqslant 1\tag{23}$$

where the volume of clusters in the RVE is shown by $V_{cluster}$. Also, μ stands for the volume fraction of cluster and η indicates the volume fraction of CNTs into the clusters. When the volume fraction of cluster is equal to RVE (μ = 1), all CNTs are uniformly scattered in the entire matrix (Fig. 2b) and there is no cluster in the matrix. However, the equality of volume of CNTs into the cluster and total volume of CNTs (η = 1) means fully agglomerated CNTs (Fig. 2c). It means that there are some clusters in the matrix so that all CNTs are located inside the clusters. If η > μ, the heterogeneity of CNTs distribution increases through an enhancement of η.

The MT approach would be applied to predict the effective elastic attributes of cluster and matrix of nanocomposite. Therefore, the effective bulk moduli K_{in} and K_{out} and the effective shear moduli G_{in} and G_{out} of inclusions and remnant parts are expressed (Syah et al., 2021):

$$K_{in}=\frac{(\delta_r-3\alpha_r K_m)\eta f_r}{3(\mu-\eta f_r+\eta f_r\alpha_r)}+K_m\tag{24a}$$

$$K_{out}=\frac{f_r(\delta_r-3K_m\alpha_r)(1-\eta)}{3[1-\mu-f_r(1-\eta)+\alpha_r f_r(1-\eta)]}+K_m\tag{24b}$$

$$G_{in}=\frac{(\eta_r-2G_m\beta_r)f_r\eta}{2(\mu+f_r\eta\beta_r-f_r\eta)}+G_m\tag{24c}$$

$$G_{out}=\frac{f_r(\eta_r-2G_m\beta_r)(1-\eta)}{2[1-f_r(1-\eta)-\mu+f_r(1-\eta)\beta_r]}+G_m\tag{24d}$$

in which

$$\alpha_r=\frac{3(K_m+G_m)+k_r-l_r}{3(k_r+G_m)}\tag{25a}$$

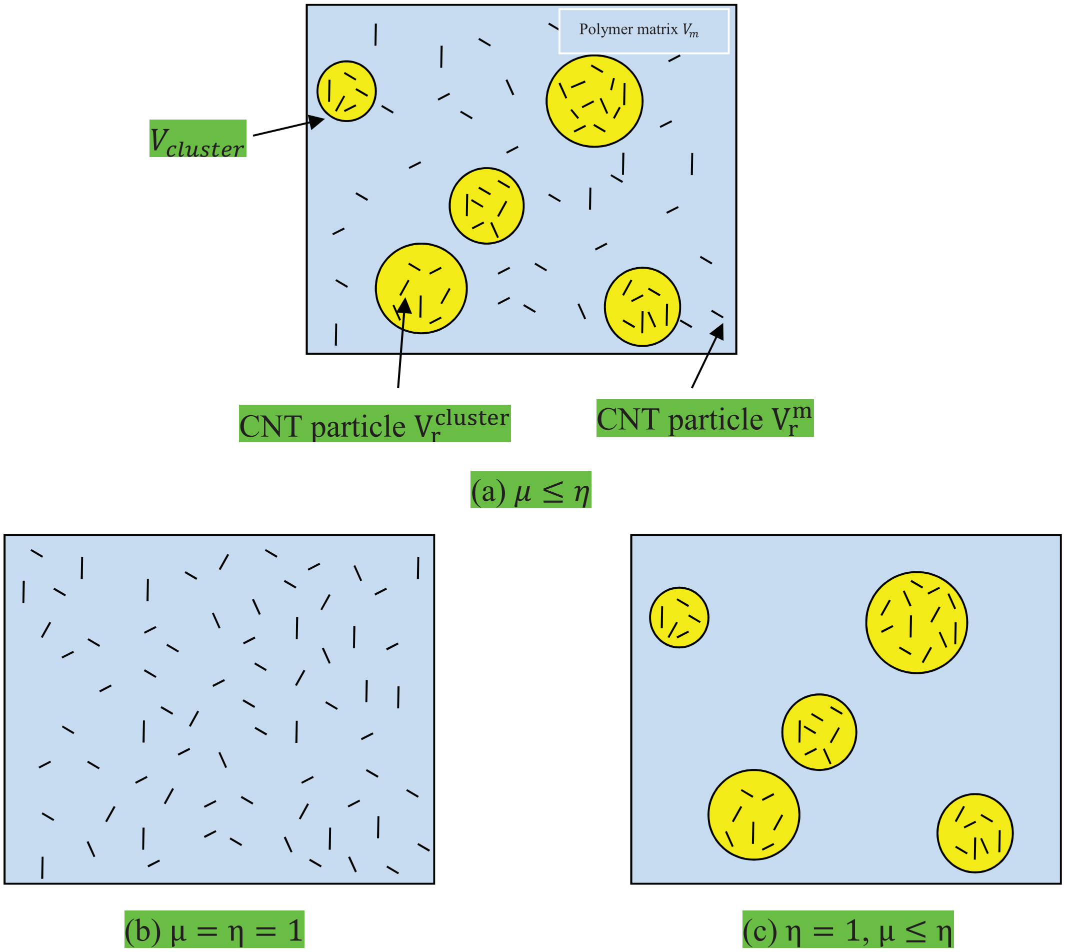

Fig. 2 Agglomeration of CNTs in a cluster model (Syah et al., 2021)

$$\beta_r = \frac{1}{5}\left\{\frac{4G_m + 2k_r + l_r}{3(k_r + G_m)} + \frac{4G_m}{G_m + p_r} + \frac{2[G_m(3K_m + G_m) + G_m(3K_m + 7G_m)]}{G_m(3K_m + G_m) + m_r(3K_m + 7G_m)}\right\} \tag{25b}$$

$$\delta_r = \frac{1}{3}\left[2l_r + n_r + \frac{(3K_m + 2G_m - l_r)(2k_r + l_r)}{G_m + k_r}\right] \tag{25c}$$

$$\eta_r = \frac{1}{5}\left[\frac{8p_r G_m}{p_r + G_m} + \frac{2}{3}(n_r - l_r) + \frac{2(2G_m + l_r)(k_r - l_r)}{3(G_m + k_r)} + \frac{8(3K_m + 4G_m)m_r G_m}{G_m(7m_r + G_m) + 3K_m(m_r + G_m)}\right] \tag{25d}$$

in which f_r represents the volume fraction of equivalent fiber. The volume fraction of equivalent fiber can be studied for various distributions of continuously graded CNT reinforced composite (CGCNTRC) which are presented in the following relations (Kamarian et al., 2013). If both inner and outer surfaces of nanocomposites are reinforced using mid-plane symmetric graded CNTs richly called symmetric CG-CNTRC. When the former is reinforced by CNTs poorly, while the latter is reinforced by CNTs richly called asymmetric CG-CNTRC (Hedayati and Sobhani Aragh, 2012).

$$Symmetric\ CGCNTRC: f_r = 4\frac{|z - h/2|}{h} f_f^* \tag{26a}$$

$$Asymmetric\ CGCNTRC: f_r = 4\frac{z}{h} f_f^* \tag{26b}$$

where f_f^* refers to volume fraction of CNTs which is obtained using mass fraction of CNTs m_f as given (Hedayati and Sobhani Aragh, 2012):

$$f_f^* = \left[\frac{\rho_r}{m_f} - \rho_r + 1\right]^{-1} \tag{27}$$

where $\rho_r = \rho_f/\rho_m$. K_m and G_m are correlated to the bulk and shear moduli of isotropic matrix within Eq. (25) which can be calculated as:

$$K_m = \frac{E_m}{3(1 - 2\upsilon_m)} \tag{28a}$$

$$G_m = \frac{E_m}{2(1 + \upsilon_m)} \tag{28b}$$

in which E_m denote the elastic modulus of matrix and υ_m indicates the Poisson's ratio of matrix. Some parameters in Eq. (25) including k_r, l_r, m_r, n_r and p_r are Hill's elastic moduli of CNTs (Kamarian et al., 2016):

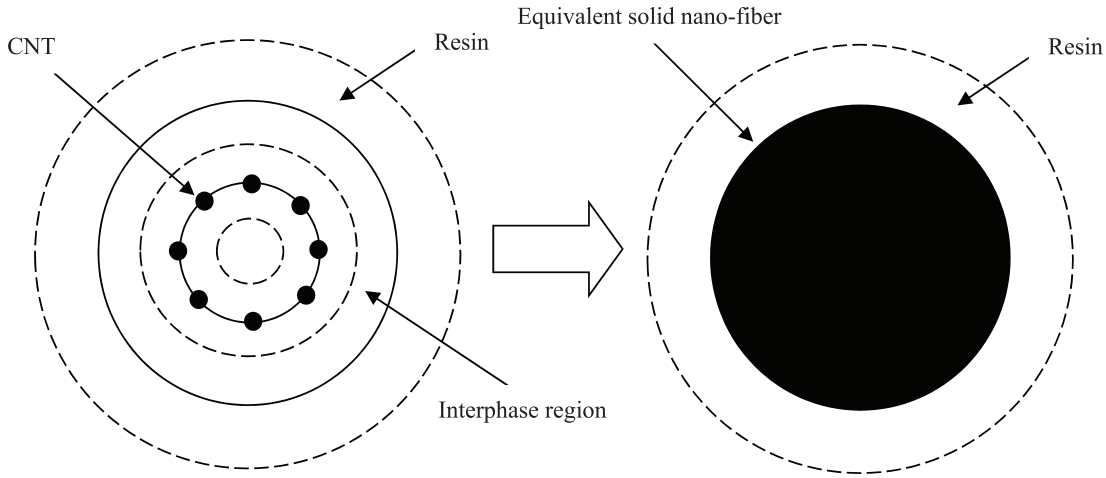

Fig. 3 Conversion strategy (Ghasemi and Mohandes, 2017)

$$C_r = \begin{bmatrix} n_r & l_r & l_r & 0 & 0 & 0 \\ l_r & k_r + m_r & k_r - m_r & 0 & 0 & 0 \\ l_r & k_r - m_r & k_r + m_r & 0 & 0 & 0 \\ 0 & 0 & 0 & p_r & 0 & 0 \\ 0 & 0 & 0 & 0 & m_r & 0 \\ 0 & 0 & 0 & 0 & 0 & p_r \end{bmatrix} \tag{29a}$$

$$C_r = \begin{bmatrix} \frac{1}{E_L} & -\frac{\upsilon_{TL}}{E_T} & -\frac{\upsilon_{ZL}}{E_Z} & 0 & 0 & 0 \\ -\frac{\upsilon_{LT}}{E_L} & \frac{1}{E_T} & -\frac{\upsilon_{ZT}}{E_Z} & 0 & 0 & 0 \\ -\frac{\upsilon_{LZ}}{E_L} & -\frac{\upsilon_{TZ}}{E_T} & \frac{1}{E_Z} & 0 & 0 & 0 \\ 0 & 0 & 0 & \frac{1}{G_{TZ}} & 0 & 0 \\ 0 & 0 & 0 & 0 & \frac{1}{G_{ZL}} & 0 \\ 0 & 0 & 0 & 0 & 0 & \frac{1}{G_{LT}} \end{bmatrix}^{-1} \tag{29b}$$

$E_L, E_T, E_Z, G_{TZ}, G_{ZL}, G_{LT}$ and υ_{LT} represent the modulus and Poisson's ratio of equivalent fiber. Via MT procedure, the equivalent bulk K and shear G modulus of nanocomposites would be computed as (Kamarian et al., 2016):

$$K = K_{out}\left[1 + \frac{\mu\left(\frac{K_{in}}{K_{out}} - 1\right)}{1 + \alpha\left(\frac{K_{in}}{K_{out}} - 1\right)(1-\mu)}\right] \tag{30a}$$

$$G = G_{out}\left[1 + \frac{\mu\left(\frac{G_{in}}{G_{out}} - 1\right)}{1 + \left(\frac{G_{in}}{G_{out}} - 1\right)\beta(1-\mu)}\right] \tag{30b}$$

$$\upsilon_{out} = \frac{3K_{out} - 2G_{out}}{2(3K_{out} + G_{out})} \tag{31a}$$

$$\alpha = \frac{1 + \upsilon_{out}}{3(1 - \upsilon_{out})} \tag{31b}$$

$$\beta = \frac{2(4 - 5\upsilon_{out})}{15(1 - \upsilon_{out})} \tag{31c}$$

Then the effective Young's modulus E and Poisson's ration υ of the composite can be defined as given (Tsai et al., 2003):

$$E = \frac{9KG}{3K + G} \tag{32a}$$

$$\upsilon = \frac{3K - 2G}{6K + 2G} \tag{32b}$$

5. Mechanical properties of CNTRCs

The mechanical characteristics of straight CNT inserted in matrix can be predicted using an equivalent solid long fiber with 2.374 nm diameter bonded to surrounding resin which is depicted in Fig. 3.

In this manuscript, the extended rule of mixture is utilized to focus on the influence of the CNTs on the properties of shell reinforced composites. Longitudinal modulus E_{LEF}, transverse modulus E_{TEF}, shear modulus G_{EF} Poisson's ratio υ_{EF}, and volume fraction V_{EF} of equivalent fiber can be obtained utilizing rule of mixture (ROM) (Shokrieh and Rafiee, 2010):

$$E_{LEF} = \frac{E_{LC}}{V_{EF}} - \frac{E_M V_M}{V_{EF}} \tag{33a}$$

$$E_{TEF} = \frac{E_{TC}}{V_{EF}} - \frac{E_M V_M}{V_{EF}} \tag{33b}$$

$$G_{EF} = \frac{G_C}{V_{EF}} - \frac{G_M V_M}{V_{EF}} \tag{33c}$$

$$\upsilon_{EF} = \frac{\upsilon_C}{V_{EF}} - \frac{\upsilon_M V_M}{V_{EF}} \tag{33d}$$

where E_{LC}, E_{TC} and G_C stand for longitudinal, transverse and shear modulus of the composites, and E_M, G_M and V_M are longitudinal modulus, shear modulus and volume fraction of the matrix, respectively. The mechanical characteristics of equivalent long fiber (Ghasemi and Mohandes, 2017) are expressed in Table 1.

6. Beam modal function model's solution:

A wide range of solution methods exist including numerical (Liu et al., 2016; Civalek, 2004; Talebitooti, 2013; Mohandes

Table 1 Equivalent long fiber properties

Mechanical properties	Equivalent fiber (Ghasemi and Mohandes, 2017)
E_{LEF}	649.12 (GPa)
E_{TEF}	11.27 (GPa)
G_{EF}	5.13 (GPa)
υ_{EF}	0.284
ρ_{EF}	1400 Kg/m^3

and Ghasemi, 2016; Ghasemi and Mohandes, 2016; Tornabene et al., 2015; Zhong and Yu, 2009; Al-Furjan et al., 2020; Al-Furjan et al., 2021; Al-Furjan et al., 2020; Al-Furjan et al., 2020; Al-Furjan et al., 2020), analytical (Bourada et al., 2020; Zhang et al., 2021; Lam and Loy, 1994; Callahan and Baruh, 1999), semi-analytical ones which are applied to analyze the vibration and dynamic of different structures. Although analytical methods are more accurate than numerical ones, various boundary conditions can be analyzed using numerical approaches. In this manuscript, beam modal function model (Mohammadimehr et al., 2016), that is a semi-analytical method with great accuracy, is utilized to consider dynamic of CNTFPML cylindrical shell with various boundary conditions. Thus, the following expression including mode shapes in the longitudinal U(x), torsional V(x) and flexural W(x) directions is assumed (Wang and Lai, 2000):

$$u(x,\theta,t) = U(x)\sin(n\theta)\sin(\omega t) \tag{34a}$$

$$v(x,\theta,t) = V(x)\cos(n\theta)\sin(\omega t) \tag{35b}$$

$$w(x,\theta,t) = W(x)\sin(n\theta)\sin(\omega t) \tag{36c}$$

in which n refers the circumferential wave numbers in the mode shape and ω denotes the natural frequency. The modal displacements are given as following based on main constants α, A, B and C (Wang and Lai, 2000; Lam and Loy, 1995):

$$\{U(x),\ V(x),\ W(x)\}^T = Ae^{\alpha z/R}\{C,\ B,\ 1\}^T \tag{35}$$

It is worth noticing that the exact value of α, which is related to boundary condition, for cylindrical shells. it should be identified using the axial modal parameter m for a given circumferential modal parameter n. The amount of α would be obtained using the following assumption: the flexural mode shapes of the cylindrical shell in the axial direction are in the identical form with the flexural vibration of beam within the same boundary limitations. Then, the beam modal function has been applied to the acquire the magnitude of α refered to proper limitations (Mahmood et al., 2021). For instance, the modal wave number would be approximately obtained through beam function model as following (Mahmood et al., 2021):

$$\alpha = \frac{m\pi}{L}\ m = 1, 2, 3, \ldots \tag{36}$$

Moreover, the α for a cylindrical shell under clamped boundary conditions would be derived by:

$$\alpha = \frac{\left(m+\frac{1}{2}\right)\pi}{L}\ m = 1, 2, 3, \ldots \tag{37}$$

Moreover, the α for a cylindrical shell with free-free boundary conditions can be given by:

$$\alpha = \frac{\left(m-\frac{1}{2}\right)\pi}{L}\ m = 2, 3, 4, \ldots \tag{38}$$

Like the Eq. (38), the modes $m = 0$ and $m = 1$ are two inextensional modes of circular cylindrical shells so that these two modes correlated to rigid body translation and rotation modes for a free-free beam. Therefore, they are trivial modes with zero frequencies for the beams and they cannot be estimated for cylindrical shells. So, the non-dimensional form of equations of motion:

$$H_{3\times3}\{C,\ B,\ 1\}^T = \{0,\ 0,\ 0\}^T \tag{39}$$

$$H_{11} = \alpha^2 - a_{66}n^2 + \frac{1}{4A_{11}R^2}\mu\ell^2h\alpha^2n^2 - \frac{1}{4A_{11}R^2}\mu\ell^2hn^4 + \Omega^2 \tag{40}$$

$$H_{12} = -H_{21} = -a_{12}n\alpha - b_{12}\frac{n\alpha}{R} - a_{66}n\alpha - 2b_{66}\frac{n\alpha}{R} - \frac{1}{4A_{11}R^2}\mu\ell^2h\alpha^3n + \frac{1}{4A_{11}R^2}\mu\ell^2h\alpha^3n^3$$

$$H_{13} = -H_{31} = a_{12}\alpha - b_{11}\frac{\alpha^3}{R} + b_{12}\frac{n^2\alpha}{R} - 2b_{66}\frac{n^2\alpha}{R}$$

$$H_{22} = a_{66}\alpha^2 + 2b_{66}\frac{\alpha^2}{R} - a_{22}n^2 - 2b_{22}\frac{n^2}{R} + b_{66}\frac{\alpha^2}{R} + 2d_{66}\left(\frac{\alpha}{R}\right)^2 - d_{22}\left(\frac{n}{R}\right)^2 - \frac{1}{4A_{11}R^2}\mu\ell^2h\alpha^4 + \frac{1}{4A_{11}R^2}\mu\ell^2h\alpha^2n^2 + \Omega^2$$

$$H_{23} = H_{32} = -2b_{66}\frac{\alpha^2n}{R} + a_{22}n - b_{12}\frac{\alpha^2n}{R} + b_{22}\frac{n^3}{R} - 2d_{66}\left(\frac{\alpha}{R}\right)^2n + b_{22}\frac{n}{R} - d_{12}\left(\frac{\alpha}{R}\right)^2n + d_{22}\frac{n^3}{R^2}$$

$$H_{33} = 2b_{12}\frac{\alpha^2}{R} - d_{11}\frac{\alpha^4}{R^2} + 2d_{12}\left(\frac{n\alpha}{R}\right)^2 + d_{66}\left(\frac{2n\alpha}{R}\right)^2 - 2b_{22}\frac{n^2}{R} - d_{22}\frac{n^4}{R^2} - a_{22} - \frac{1}{2A_{11}}\mu\ell^2h\left(-\frac{1}{2}\frac{\alpha^2n^2}{R^2} + \frac{5}{2}\frac{n^4}{R^2}\right) + \Omega^2$$

$$a_{12} = \frac{A_{12}}{A_{11}}\ a_{22} = \frac{A_{22}}{A_{11}}\ a_{66} = \frac{A_{66}}{A_{11}}\ b_{11} = \frac{B_{11}}{A_{11}}\ b_{12} = \frac{B_{12}}{A_{11}}\ b_{22} = \frac{B_{22}}{A_{11}} \tag{41}$$

$$b_{66} = \frac{B_{66}}{A_{11}}\ d_{11} = \frac{D_{11}}{A_{11}}\ d_{12} = \frac{D_{12}}{A_{11}}\ d_{22} = \frac{D_{22}}{A_{11}}\ d_{66} = \frac{D_{66}}{A_{11}}\ \Omega = \omega\sqrt{\frac{\rho hR^2}{A_{11}}}$$

7. Numerical results and discussion

The work is focused on an investigation of the agglomeration effects on free vibration of micro CNTFPML cylindrical shells in terms of semi-analytical approach. It should be noted that the composite sector of FML cylindrical shell is reinforced by agglomerated CNTs so that this section is combined to thin metal layers. Initially, the non-dimensional frequencies $\Omega = \omega\sqrt{(\rho R^2/E)}$ of classical macro CNTFPML cylindrical should has been compared to other research study (Syah et al., 2021) in Table 2. Material characteristics of CNTFPML cylindrical shell used in this case is CARALL reinforced by CNTs for n = 1 and m = 1. The geometric characteristics of cylindrical shell are considered $L = 10 \times R$; $R = 23.437$. It can be found out that the presented results in this investigation compare excellent with the results of Ghasemi et al. (Syah et al., 2021). Besides, the non-dimensional frequencies of the presented study would be compared with the frequency form $\Omega = R\omega\sqrt{(1-\upsilon^2)\rho/E}$ of the other research which are isotropic macro cylindrical shells with different boundary conditions. That is worth noticing the material properties of studied isotropic cylindrical shell are $\upsilon = 0.3$ and $E = 200\,\mathrm{GPa}$. In addition, the cylindrical shell geometry to compare with wave propagation method illustrated below via Table 3, $h/R = 0.002$ and $L/R = 20$ and for comparison with Ritz procedure presented in Table 4 are $h/R = 0.01$ and $L/R = 20$. The outputs illustrate excellent correlation among the method illustrated in this manuscript and wave propagation and Ritz procedures.

Next, the CNTFPML cylindrical shell with considering agglomeration impacts is studied with the following circumstances:

The metal layers are constructed using aluminum and the composite layers are consisting of carbon/epoxy with cross-ply lay-ups $[\mathrm{Al}/0^{\circ}/90^{\circ}/0^{\circ}]$. Also, geometric attributes of cylindrical shell are considered $L = 10 \times R$, $\ell = 0.0937 \times 10^{-6}$, $R = 23.437 \times 10^{-6}$ subjected to simply supported boundary condition. Moreover, the agglomerated CNTs are distributed within the resin symmetrically. Further, the mechanical properties of fiber, metal, CNT and matrix utilized in this manuscript are presented in Table 5.

In the following expressions, the sensitivity of vibration response for different items is presented for the agglomerated micro CNTFPML cylindrical shell which are the agglomeration, the material length scale parameter, the distribution of CNTs referred to various boundary situation, the dimensions of cylindrical shell, the material attributes, the mass fraction of fiber, and the circumferential wave numbers.

Table 2 The dimensionless frequencies of CNTFPML classical cylindrical shell for differing agglomeration parameters

μ	Non-dimensional frequency							
	Ref. (Syah et al., 2021)				Present			
	$\eta = 0.2$	$\eta = 0.3$	$\eta = 0.4$	$\eta = 0.5$	$\eta = 0.2$	$\eta = 0.3$	$\eta = 0.4$	$\eta = 0.5$
0.1	0.300	0.298	0.295	0.291	0.300	0.298	0.295	0.291
0.2	0.306	0.304	0.301	0.298	0.306	0.304	0.301	0.298
0.3	0.312	0.310	0.308	0.304	0.312	0.310	0.308	0.304
0.4	0.318	0.317	0.314	0.311	0.318	0.317	0.314	0.311
0.5	0.324	0.323	0.321	0.319	0.324	0.323	0.321	0.319

Table 3 The dimensionless frequencies of an isotropic circular cylindrical shell for various boundary conditions ($m = 1$, $h/R = 0.002$ and $L/R = 20$).

n	Boundary condition					
	Clamped-clamped			Simply supported		
	Present method	Ref. (Lam and Loy, 1995)	Difference (%)	Present method	Ref. (Lam and Loy, 1995)	Difference (%)
1	0.0349	0.0344	1.376	0.01610	0.01610	0.0006
2	0.0118	0.0120	2.381	0.005454	0.005453	0.0135
3	0.0071	0.0072	1.934	0.005042	0.005041	0.0194

Table 4 The dimensionless frequencies of an isotropic cylindrical shell for various boundary conditions ($m = 1$, $h/R = 0.01$ and $L/R = 20$).

n	Boundary condition								
	Clamped-clamped			Clamped-simply			Simply supported		
	Present method	Ref. Zhang et al., 2001	Difference (%)	Present method	Ref. Zhang et al., 2001	Difference (%)	Present method	Ref. Zhang et al., 2001	Difference (%)
1	0.03489	0.03488	0.003	0.02472	0.02472	0.0081	0.01610	0.01610	0.012
2	0.01406	0.01405	0.071	0.01129	0.01128	0.0709	0.00939	0.00938	0.064
3	0.02273	0.02272	0.031	0.02234	0.02233	0.0179	0.02211	0.02210	0.014
4	0.04227	0.04227	0.009	0.04217	0.04216	0.0047	0.04210	0.04209	0.002

Table 5 Material attributes of micro CNTFPML cylindrical shell (Yang et al., 2002)

Material attributes				
CNT	Fiber		Matrix	Metal (Aluminum)
	Carbon	Glass		
$E_{11}^{CN} = 5.6466\,(\mathrm{TPa})$	$E_{11f} = 230\,(GPa)$	$E_{11f} = 35\,(GPa)$	$E_{old}^{m} = 2.5\,(GPa)$	$E^{metal} = 72.4\,(GPa)$
$E_{22}^{CN} = 7.080\,(\mathrm{TPa})$	$E_{22f} = 8\,(GPa)$	$E_{22f} = 5\,(GPa)$	$\rho_{old}^{m} = 1150\,(Kg/m^3)$	$\rho^{metal} = 2700\,(Kg/m^3)$
$G_{12}^{CN} = 1.9445\,(\mathrm{TPa})$	$G_f = 27.3\,(GPa)$	$G_f = 7.17(GPa)$	$\upsilon_{old}^{m} = 0.34$	$\upsilon^{metal} = 0.33$
$\rho^{CN} = 1400\,(Kg/m^3)$	$\rho_f = 1750\,(Kg/m^3)$	$\rho_f = 2500\,(Kg/m^3)$		
$\upsilon_{12}^{CN} = 0.175$	$\upsilon_f = 0.256$	$\upsilon)_f = 0.27$		

The first investigation deals with the consideration of the sequel of material length scale parameter on the vibration response of agglomerated CNTFPML cylindrical shell with respect to variations of length and radius. As visible in Fig. 4, increased value of ℓ leads to growing the magnitude of dimensionless frequencies of micro CNTFPML cylindrical shell. It shows that the more the material length scale parameter impact enhances, the greater the frequencies of shell grow. Nevertheless, with raising the length-to-radius ratio, the frequencies gradually decline so that they tend to convergence for long lengths for various ℓ. The reason for convergence of these curves is the raise of length so that as the length of cylindrical shell increases, the effects of material length scale on the frequencies of agglomerated CNTFPML micro cylindrical shell decreases.

Fig. 5 plots the seques of agglomeration parameters on the non-dimensional frequencies of micro CNTFPML cylindrical shell. All the curves show a mildly increase of dimensionless frequencies for growing amounts of μ with a reducing magnitude of η. The figure illustrates that the agglomeration parameters have a considerable influence on the micro phase so that as the volume fraction of cluster grows, the agglomeration effects decline which lead to rising the frequencies that is positive. It is worth mentioning that when the volume fraction of cluster enhances, it causes the value of CNTs agglomeration decreases which results in more stiffness of the structure and then growth of frequencies. Nevertheless, through enhancing the volume fraction of CNTs inside the cluster, which causes increasing the agglomeration impacts, the frequencies drop which is negative aspect. The reason for decrease of the frequencies is the fact that the more the CNTs agglomerate inside a cluster, the more the stiffness of the structure declines because the homogeneity of the CNTs into the matrix decreases and CNTs concentrate in a cluster.

Fig.6 illustrates the variation of dimensionless frequencies with the consideration of material length scale parameter for various values of agglomeration parameters. As depicted in the figure, increased values of μ and η altogether resulted in growing the dimensionless frequencies of micro cylindrical shell. Although, as predicted in the previous figure, with increasing the values of μ and η separately, the frequencies raise and drop, respectively, the present graph shows that growing both amounts of μ and η together leads to increasing magnitude of frequency. Therefore, the influence of μ on the frequencies of micro CNTFPML cylindrical shell is more than η. In addition, increasing value of h/ℓ means that the influence of material length scale parameter drops which leads to decreasing the rigidity of micro cylindrical shell and finally declining the values of frequencies.

Fig. 7 shows the sensitivity of the structural frequencies with thickness-to-radius ratio for various amounts of agglomeration parameter μ, through keeping constant parameter η.

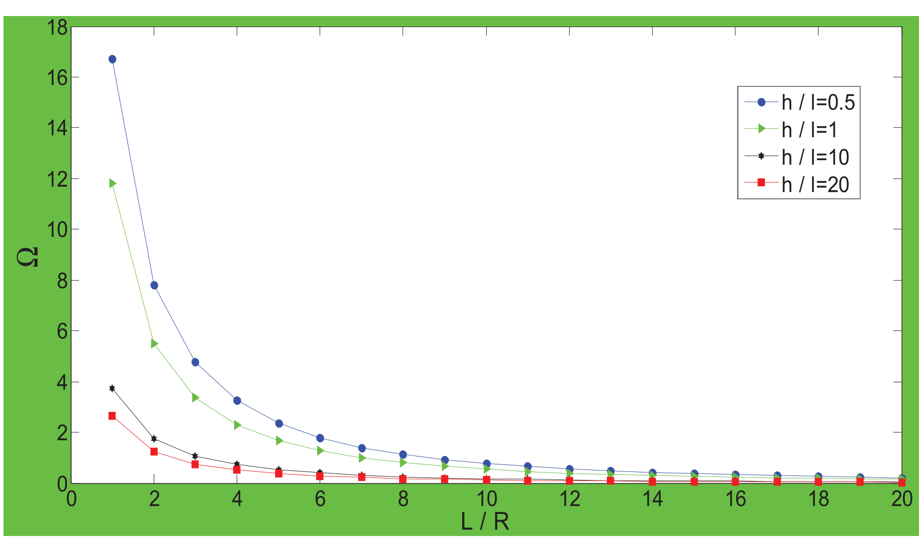

Fig. 4 The dimensionless frequencies of agglomerated micro CNTFPML cylindrical shell versus L/R for various magnitudes ofh/ℓ

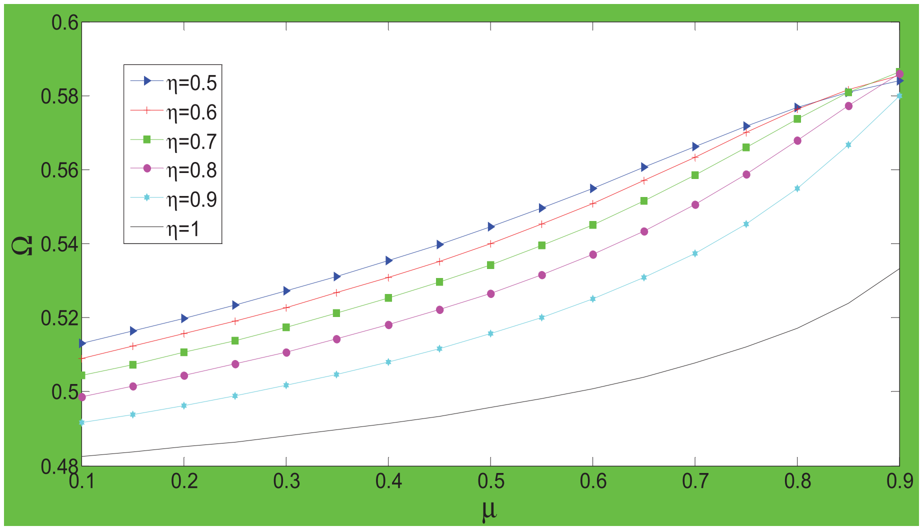

Fig. 5 The dimensionless frequencies of agglomerated micro CNTFPML cylindrical shell versus μ for various magnitudes ofη

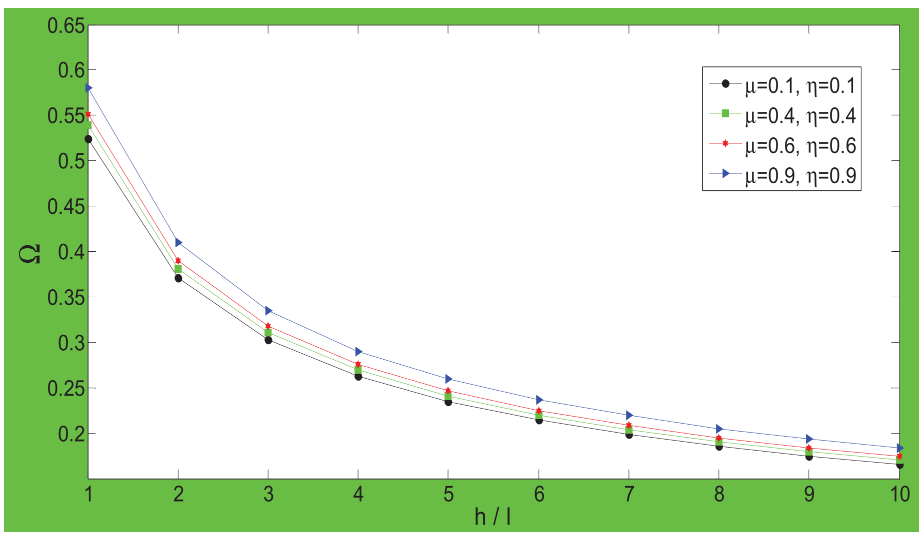

Fig. 6 Dimensionless frequencies of agglomerated micro CNTFPML cylindrical shell versus h/ℓ for various agglomeration parameters

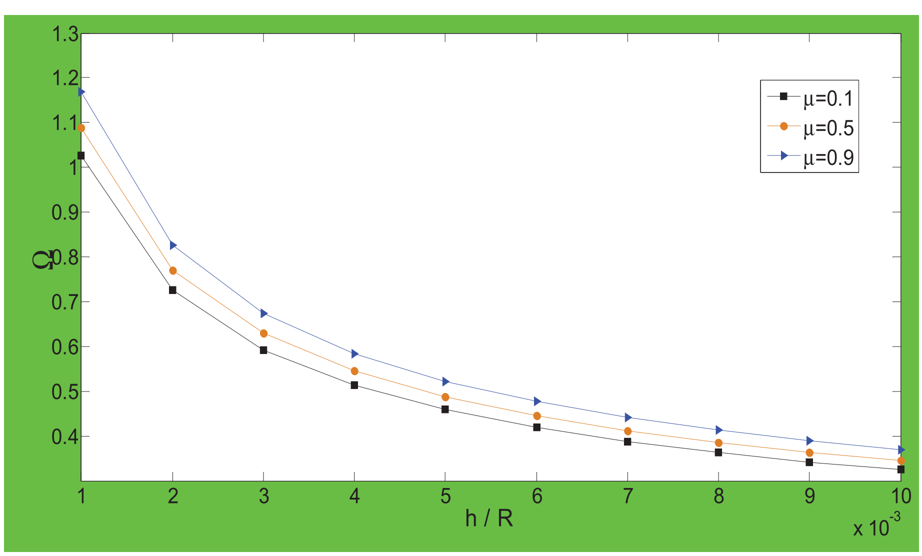

Fig. 7 The dimensionless frequencies of agglomerated micro CNTFPML cylindrical shell versus h/R for various magnitudes ofμ

Considering graphs of Fig. 7, the frequencies of micro agglomerated CNTFPML cylindrical shell with growing the agglomeration attributes increase gradually like μ is raised. Moreover, the graphs vividly indicate a monotone decline of non-dimensional frequencies when dimensionless magnitude h/R is increased.

In Fig. 8, the effects of distribution of CNTs and boundary conditions are shown on the dimensionless frequencies of micro agglomerated CNTFPML cylindrical shell for differing magnitudes of dimensionless parameter h/R for the constant amounts of agglomeration parameters μ and η and $n = 1$ and $m = 2$. It is worth saying that the structural frequencies of symmetric distribution of CNTs are greater than asymmetric one since asymmetric distribution yields decreasing the stiffness of the structure. As the CNTs distributed symmetrically, the homogeneous of the structure maintains, which causes greater stiffness, that leads to more frequencies. Once again, the dimensionless frequencies of clamped boundary condition for both symmetric and asymmetric distributions are remarkably greater than the other ones related to simply supported and free-free boundary limitations. It is illustrated the frequencies of free-free boundary condition are less than other literatures since there is not any constraint in the boundary limitations. Then, the frequencies slope of micro cylindrical shell decline moderately for an increased value of h/R.

As clearly shown in Fig. 9, a higher effect of vibration response can be found in a structure constructed of carbon fibers in comparison with glass one. Although the dimensionless frequencies increase gradually for both materials with growing agglomeration parameter, the slope change of glass-based composites is a bit more than carbon fiber composite materials. Specially it could be seen that with growing agglom-

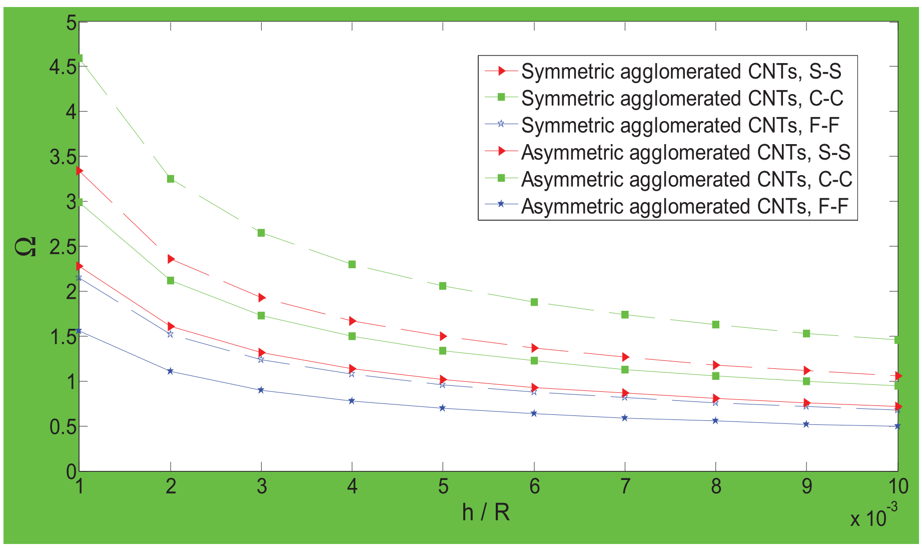

Fig. 8 The dimensionless frequencies of agglomerated micro CNTFPML cylindrical shell versus h/R for various distributions of CNTs and boundary conditions

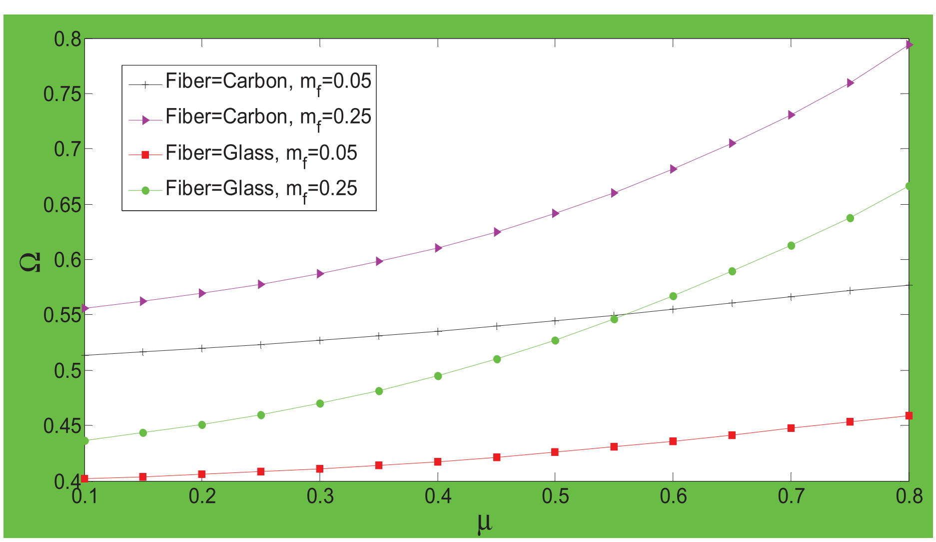

Fig. 9 The dimensionless frequencies of agglomerated micro CNTFPML cylindrical shell versus μ for various fiber materials and mass fraction of fiber

eration parameter, the curve slope of carbon-based composites for $m_f = 0.05$ decrease and the frequencies reaches about 0.57 in the $\mu = 0.8$. Furthermore, according to the curves, the natural frequencies for mass fraction of fiber equal to 0.25 assume a higher value than the ones made of 0.05 mass fraction. Also, based on the figures, the frequencies variations of $m_f = 0.25$ are significantly greater than $m_f = 0.05$ with respect to a growing value of μ since through enhancing the volume fraction of fiber, the volume fraction of reinforced matrix reduses then leads to the stiffness drop of the whole structure.

Possible impacts of agglomeration parameters and circumferential wave number on the dimensionless frequencies of micro CNTFPML cylindrical shells are represented in Fig. 10. This plot reveals higher difference of the frequencies of agglomerated cylindrical shell for greater amounts of n. It is worth noticing that enhancing the circumferential wave number results in a reduction of structural frequency initially and then moderate increase. As predicted, by decreasing the concentration of CNTs within a cluster, the natural frequencies are increased.

Fig. 11 compares the dimensionless frequencies of micro agglomerated CNTFPML cylindrical shells vs. volume fraction of CNTs for various values of agglomeration parameter μ with keeping constant parameter η equal to 1. Based on the figure, the frequency changes are greater for lower values of f_f, even though these variations are more visible with growing the cluster volume. Also, as the volume fraction of CNTs enhances, the sensitivity of vibration response raises at first, and then it reaches almost a stable trend. The least variations occur in $\mu = 0.2$ so that it shows almost a stable trend around $\Omega = 0.485$. It has been resulted to the lower the volume fraction of cluster, the less the variations of vibration. This is since

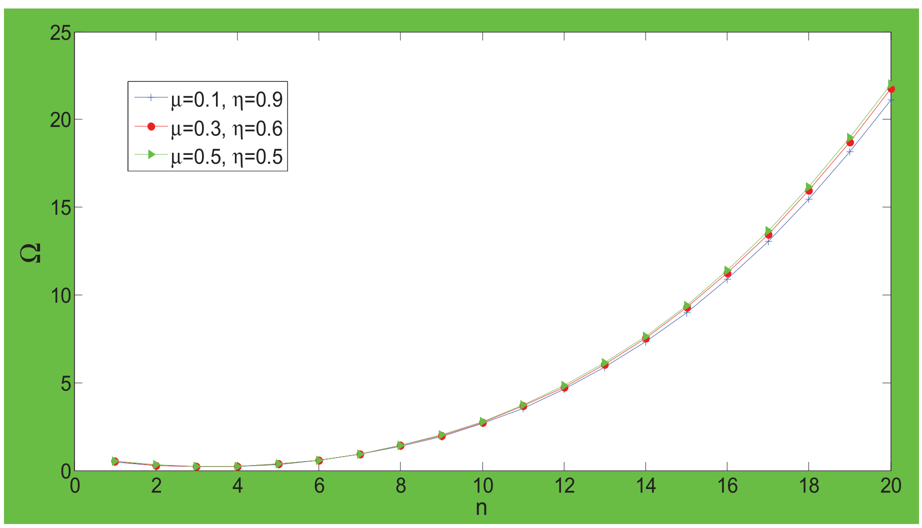

Fig. 10 The dimensionless frequencies of agglomerated micro CNTFPML cylindrical shell versus n for various agglomeration parameters

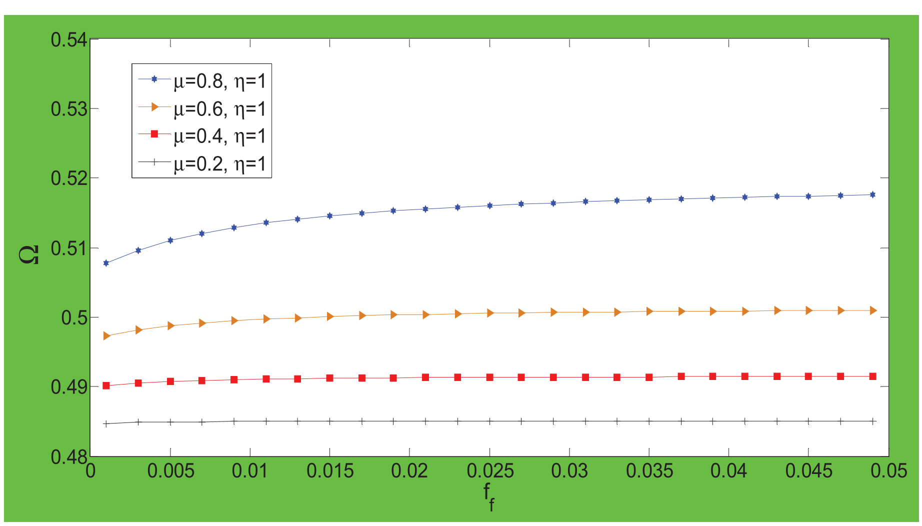

Fig. 11 The dimensionless frequencies of agglomerated micro CNTFPML cylindrical shell versus volume fraction of CNTs for various agglomeration parameter μ.

the less cluster could affect less the stiffness of the structure even if the magnitudes of CNTs would be the same in different clusters.

8. Conclusion

The presented manuscript has been developed for obtaining the frequencies of micro agglomerated CNTFPML cylindrical shell via MCST. The equations of motion are obtained through framework of Love's first approximation theory and Hamilton's principle and solved using the beam modal function model for various boundary conditions. Moreover, the effective elastic properties of nanocomposites are determined utilizing MT approach. The findings can be illustrated as:

1. The material length scale parameter influenced significantly on the natural frequencies of micro CNTFPML cylindrical shell. The dimensionless frequencies of the micro shell increased via enhancing the amount of ℓ, while they decreased mildly with raising the length-to-radius ratio. The frequencies of greater length-to-radius ratios reached stable values subjected to various material length scale parameters.
2. The sensitivity of vibration response to agglomeration parameters was more pronounced so that the dimensionless frequencies of micro CNTFPML cylindrical shell increased gradually through rising the volume fraction of cluster. A negative influence of agglomeration was growing the volume fraction of CNTs within the cluster which lead to frequency decline.
3. An increased value of agglomeration parameters together yielded a growth in the natural frequencies of micro CNTFPML cylindrical shell. This showed that compared to η, the impacts of μ on the vibration response of micro CNTFPML cylindrical shell was more effective.
4. Results obtained for symmetric and asymmetric distributions of CNTs are quite different for keeping values of μ and η constant. Symmetric distribution of CNTs leads to much higher magnitudes of frequencies in comparison with asymmetric one particularly for clamped boundary conditions.

Declaration of Competing Interest

The authors declare that they have no known competing financial interests or personal relationships that could have appeared to influence the work reported in this paper.

References

Afshari, H., Amirabadi, H., 2021. Vibration characteristics of rotating truncated conical shells reinforced with agglomerated carbon nanotubes. J. Vib. Control. https://doi.org/10.1177/10775463211000499.

Akgoz, B., Civalek, O., 2011. Strain gradient elasticity and modified couple stress models for buckling analysis of axially loaded micro-scaled beams. Int. J. Eng. Sci. 49, 1268–1280.

Akgoz, B., Civalek, O., 2016. Bending analysis of embedded carbon nanotubes resting on an elastic foundation using strain gradient theory. Acta Astronaut. 119, 1–12.

Al-Furjan, M.S.H., Safarpour, H., Habibi, M., Safarpour, M., Tounsi, A., 2020. A comprehensive computational approach for nonlinear thermal instability of the electrically FG-GPLRC disk based on GDQ method. Eng. Comput. https://doi.org/10.1007/s00366-020-01088-7.

Al-Furjan, M.S.H., Habibi, M., Ni, J., Jung, D.W., Tounsi, A., 2020. Frequency simulation of viscoelastic multi-phase reinforced fully symmetric systems. Eng. Comput. https://doi.org/10.1007/s00366-020-01200-x.

Al-Furjan, M.S.H., Habibi, M., Jung, D.W., Sadeghi, S., Safarpour, H., Tounsi, A., Chen, G., 2020. A computational framework for propagated waves in a sandwich doubly curved nanocomposite panel. Eng. Comput. https://doi.org/10.1007/s00366-020-01130-8.

Al-Furjan, M.S.H., Habibi, M., Rahimi, A., Chen, G., Safarpour, H., Safarpour, M., Tounsi, A., 2020. Chaotic simulation of the multi-phase reinforced thermo-elastic disk using GDQM. Eng. Comput. https://doi.org/10.1007/s00366-020-01144-2.

Al-Furjan, M.S.H., Hatami, A., Habibi, M., Shan, L., Tounsi, A., 2021. On the vibrations of the imperfect sandwich higher-order disk with a lactic core using generalize differential quadrature method. Compos. Struct. 257, 113150.

Allahkarami, F., Nikkhah-Bahrami, M., 2017. The effects of agglomerated CNTs as reinforcement on the size-dependent vibration of embedded curved microbeams based on modified couple stress theory. Mech. Adv. mater. Struct. 25, 995–1008.

Arshid, E., Khorasani, M., Soleimani-Javid, Z., Amir, S., Tounsi, A., 2021. Porosity-dependent vibration analysis of FG microplates embedded by polymeric nanocomposite patches considering hygrothermal effect via an innovative plate theory. Eng. Comput. https://doi.org/10.1007/s00366-021-01382-y.

Baghlani, A., Khayat, M., Dehghan, S.M., 2020. Free vibration analysis of FGM cylindrical shells surrounded by Pasternak elastic foundation in thermal environment considering fluid-structure interaction. Applied. Math. Modelling. 78, 550–575.

Behdinan, K., Moradi-Dastjerdi, R., Safaei, B., Qin, Z., Chu, F., Hui, D., 2020. Graphene and CNT impact on heat transfer response of nanocomposite cylinders. De Gruyter. 9, 41–52.

Bendenia, N., Zidour, M., Bousahla, A.A., Bourada, F., Tounsi, A., Benrahou, K.H., Bedia, E.A., Mahmoud, S.R., Tounsi, A., 2020. Deflections, stresses and free vibration studies of FG-CNT reinforced sandwich plates resting on Pasternak elastic foundation. Comput. Conc. 26, 213–226.

Beni, Y.T., Mehralian, F., Zeighampour, H., 2016. The modified couple stress functionally graded cylindrical thin shell Formulation. Mech. Advanced. Mater. Struct. 23, 791–801.

Bourada, F., Bousahla, A.A., Tounsi, A., Bedia, E.A.A., Mahmoud, S.R., Benrahou, K.H., Tounsi, A., 2020. Stability and dynamic analyses of SW-CNT reinforced concrete beam resting on elastic-foundation. Comput. Conc. 25, 485–495.

Bousahla, A.A., Bourada, F., Mahmoud, S.R., Tounsi, A., Algarni, A., Bedia, E.A.A., Tounsi, A., 2020. Buckling and dynamic behavior of the simply supported CNT-RC beams using an integral-first shear deformation theory. Comput. Conc. 25, 155–166.

Callahan, J., Baruh, H., 1999. A closed form solution procedure for circular cylindrical shell vibrations. Int. J. Solids. Struct. 36, 2973–3013.

Chakraborty, S., Dey, T., Kumar, R., 2019. Stability and Vibration Analysis of CNT-Reinforced Functionally Graded Laminated Composite Cylindrical Shell Panels using Semi- Analytical Approach. Compos. Part B. Eng. 168, 1–14.

Chen, F., Jin, Z., Wang, E., Wang, L., Jiang, Y., Guo, P., Gao, X., He, X., 2021. Relationship model between surface strain of concrete and expansion force of reinforcement rust. Sci. Rep. 11, 4208.

Chen, F., Zhong, Y., Gao, X., Jin, Z., Wang, E., Zhu, F., Shao, X., He, X., 2021. Non-uniform model of relationship between surface strain and rust expansion force of reinforced concrete. Sci. Rep. 11, 8741.

Civalek, O., 2004. Application of differential quadrature (DQ) and harmonic differential quadrature (HDQ) for buckling analysis of thin isotropic plates and elastic columns. Eng. Struct. 26, 171–186.

Dabbagh, A., Rastgoo, A., Ebrahimi, F., 2020. Thermal buckling analysis of agglomerated multiscale hybrid nanocomposites via a refined beam theory. Mech. Based. Design. Struct. Mach. 49, 403–429.

Daghigh, H., Daghigh, V., 2019. Free Vibration of Size and Temperature-Dependent Carbon Nanotube (CNT)-Reinforced Composite Nanoplates With CNT Agglomeration. Polymer. Compos. 40, E1479–E1494.

Ebrahimi, N., Beni, Y.T., 2016. Electro-mechanical vibration of nanoshells using consistent size-dependent piezoelectric theory. Steel Compos. Struct. 22, 1301–1336.

Ebrahimi, F., Dabbagh, A., Rastgoo, A., 2019. Free vibration analysis of multi-scale hybrid nanocomposite plates with agglomerated nanoparticles. Mech. Based. Design. Struct. Mach. 49, 487–510.

Ebrahimi, F., Seyfi, A., 2021. Wave propagation response of multi-scale hybrid nanocomposite shell by considering aggregation effect of CNTs. Mech. Based. Design. Struct. Mach. 49, 59–80.

Ebrahimi, F., Seyfi, A., Dabbagh, A., 2019. Wave dispersion characteristics of agglomerated multi-scale hybrid nanocomposite beams. J. Strain. Analys. Eng. Design. 54, 276–289.

Fu, Y., Chen, Y., Zhong, J., 2014. Analysis of nonlinear dynamic response for delaminated fiber–metal laminated beam under unsteady temperature field. J. Sound. Vib. 333, 5803–5816.

Fu, Y.M., Shao, X.F., 2014. Dynamic Response of the Fiber Metal Laminated (FML) Plate with Interfacial Damage in Unstable Temperature Field. Applied. Mech. Mater. 490, 403–411.

García-Macías, E., Castro-Triguero, R., 2018. Coupled effect of CNT waviness and agglomeration: A case study of vibrational analysis of CNT/polymer skew plates. Compos. Struct. 193, 87–102.

Ghasemi, A.R., Mohandes, M., 2016. The effect of finite strain on the nonlinear free vibration of a unidirectional composite Timoshenko beam using GDQM. Adv. Aircraft. Spacecraft. Sci. 4, 379–397.

Ghasemi, A.R., Mohandes, M., 2016. Size-dependent bending of geometrically nonlinear of micro-laminated composite beam based on modified couple stress theory. Mech. Adv. Compos. Struct. 3, 53–62.

Ghasemi, A.R., Mohandes, M., 2017. Nonlinear free vibration of laminated composite Euler-Bernoulli beams based on finite strain using generalized differential quadrature method. Mech. Adv. Mater. Struct. 24, 917–923.

Ghasemi, A.R., Mohandes, M., Dimitri, R., Tornabene, F., 2019. Agglomeration effects on the vibrations of CNTs/fiber/polymer/metal hybrid laminates cylindrical shell. Compos. Part B. Eng. 167, 700–716.

Ghasemi, A.R., Mohandes, M., 2019. Comparison between the frequencies of FML and composite cylindrical shells using beam modal function model. J. Comput. Applied. Mech. 50, 239–245.

Ghasemi, A.R., Mohandes, M., 2019. Free vibration analysis of rotating fiber–metal laminate circular cylindrical shells. J. Sandwich Struct. Mater. 21 (3), 1009–1031.

Ghasemi, A.R., Mohandes, M., 2020. Free vibration analysis of micro and nano fiber-metal laminates circular cylindrical shells based on modified couple stress theory. Mech. Adv. Mater. Struct. 27, 43–54.

Ghasemi, A.R., Mohandes, M., 2019. A new approach for determination of interlaminar normal/shear stresses in micro and nano laminated composite beams. Adv. Struct. Eng. 22, 2334–2344.

Guo, X.Y., Zhang, W., 2016. Nonlinear Vibrations of a Reinforced Composite Plate with Carbon Nanotubes. Compos. Struct. 135, 96–108.

Habibi, B., Beni, Y.T., Mehralian, F., 2019. Free vibration of magneto-electro-elastic nanobeams based on modified couple stress theory in thermal environment. Mech. Adv. Mater. Struct. 26, 601–613.

Hadjesfandiari, A.R., Dargush, G.F., 2018. An assessment of higher gradient theories from a continuum mechanics perspective. arXiv. Preprint. arXiv. 1810.06977.

Hadjesfandiari, A.R., Hajesfandiari, A., Dargush, G.F., 2016. Pure plate bending in couple stress theories. arXiv. Preprint. arXiv. 1606.02954.

Hedayati, H., Sobhani Aragh, B., 2012. Influence of graded agglomerated CNTs on vibration of CNT-reinforced annular sectorial plates resting on Pasternak foundation. Appl. Math. Comput. 218, 8715–8735.

Heidari, F., Taheri, K., Sheybani, M., Janghorban, M., Tounsi, A., 2021. On the mechanics of nanocomposites reinforced by wavy/defected/aggregated nanotubes. Steel. Compos. Struct. 38, 533–545.

Huang, Y., Karimi, D., Tounsi, A., 2021. Static stability analysis of carbon nanotube reinforced polymeric composite doubly curved micro-shell panels. Arch. Civil. Mech. Eng. 21, 139.

Iriondo, J., Aretxabaleta, L., Aizpuru, A., 2015. Characterisation of the elastic and damping properties of traditional FML and FML based on a self-reinforced polypropylene. Compos. Struct. 131, 47–54.

Kamarian, S., Pourasghar, A., Yas, M.H., 2013. Eshelby-Mori-Tanaka approach for vibrational behavior of functionally graded carbon nanotube-reinforced plate resting on elastic foundation. J. Mech. Sci. Technol. 27, 3395–3401.

Kamarian, S., Salim, M., Dimitri, R., Tornabene, F., 2016. Free vibration analysis of conical shells reinforced with agglomerated carbon nanotubes. Int. J. Mech. Sci. 108–109, 157–165.

Khalili, S.M.R., Malekzadeh, K., Davar, A., Mahajan, P., 2010. Dynamic response of pre-stressed fibre metal laminate (FML) circular cylindrical shells subjected to lateral pressure pulse loads. Compos. Struct. 92, 1308–1317.

Khayat, M., Poorveis, D., Moradi, S., 2017. Semi-Analytical Approach in Buckling Analysis of Functionally Graded Shells of Revolution Subjected to Displacement Dependent Pressure. J. Pressure Vessel Technol. 139, 061202.

Khayat, M., Rahnema, H., Baghlani, A., Dehghan, S.M., 2019. A theoretical study of wave propagation of eccentrically stiffened FGM plate on Pasternak foundations based on higher-order shear deformation plate theory. Materialstoday. Communicat. 20, 100595.

Khayat, M., Baghlani, A., Dehghan, S.M., 2020. A semi-analytical boundary method in investigation of dynamic parameters of functionally graded storage tank. J. Brazilian. Society. Mech. Sci. Engin. 42, 332.

Khayat, M., Baghlani, A., Najafgholipour, M.A., 2021. The propagation of uncertainty in the geometrically nonlinear responses of smart sandwich porous cylindrical shells reinforced with graphene platelets. Compos. Struct. 258, 113209.

Khayat, M., Baghlani, A., Dehghan, S.M., Najafgholipour, M.A., 2021. The influence of graphene platelet with different dispersions on the vibrational behavior of nanocomposite truncated conical shells. Steel. Compos. Struct. 38, 47–66.

Khayat, M., Baghlani, A., Dehghan, S.M., Najafgholipour, M.A., 2021. The effect of uncertainty sources on the dynamic instability of CNT-reinforced porous cylindrical shells integrated with piezoelectric layers under electro-mechanical loadings. Compos. Struct. 273, 114336.

Khayat, M., Baghlani, A., Dehghan, S.M., Najafgholipour, M.A., 2021. The probabilistic dynamic stability analysis of fluid-filled porous cylindrical shells reinforced with graphene platelets. Thin-Walled. Struct. 167, 108256.

Khayat, M., Baghlani, A., Dehghan, S.M., Najafgholipour, M.A., 2022. Geometrically nonlinear dynamic analysis of functionally graded porous partially fluid-filled cylindrical shells subjected to exponential loads. J. Vib. Control. 28, 758–772.

Lam, K.Y., Loy, C.T., 1994. On vibrations of thin rotating laminated composite cylindrical shells. Compos. Eng. 4, 1153–1167.

Lam, K.Y., Loy, C.T., 1995. Effect of boundary conditions on frequencies of a multi-layered cylindrical shell. J. Sound. Vib. 188, 363–384.

Lee, Y.S., Kim, Y.W., 1998. Vibration analysis of rotating composite cylindrical shells with orthogonal stiffeners. Compos. Struct. 69, 271–281.

Li, H., Wang, Z., Lv, H., Zhou, Z., Han, Q., Liu, J., Qin, Z., 2020. Nonlinear vibration analysis of fiber reinforced composite cylindrical shells with partial constrained layer damping treatment. Thin-Walled Struct. 157, 107000.

Li, H., Lv, H., Gu, J., Xiong, J., Han, Q., Liu, J., Qin, Z., 2021. Nonlinear vibration characteristics of fibre reinforced composite cylindrical shells in thermal environment. Mech. System. Signal. Proc. 156, 107665.

Li, H., Lv, H., Sun, H., Qin, Z., Xiong, J., Han, Q., Liu, J., Wang, X., 2021. Nonlinear vibrations of fiber-reinforced composite cylindrical shells with bolt loosening boundary conditions. J. Sound. Vib. 496, 115935.

Li, Y., Qin, Z., Chu, F., 2021. Nonlinear forced vibrations of FGM sandwich cylindrical shells with porosities on an elastic substrate. Nonlinear Dyn. 104, 1007–1021.

Liu, B., Ferreira, A.J.M., Xing, Y.P., Neves, A.M.A., 2016. Analysis of functionally graded sandwich and laminated shells using a layerwise theory and a differential quadrature finite element method. Compos. Struct. 136, 546–553.

Liu, S., Ke, Y., Davar, A., Beni, M.H., Jam, J.E., Lutfor, R., Sarjadi, M.S., 2022. The effects of rotation on the frequencies and critical speed of CNTs/fiber/polymer/metal laminates cylindrical shell. Arabian. J. Chemist. 15, 103575.

Liu, Y., Qin, Z., Chu, F., 2021. Nonlinear forced vibrations of functionally graded piezoelectric cylindrical shells under electric-thermo-mechanical loads. Int. J. Mech. Sci. 201, 106474.

Liu, C., Zhao, Y., Wang, Y., Zhang, T., Jia, H., 2021. Hybrid Dynamic Modeling and Analysis of High-Speed Thin-Rimmed Gears. ASME. J. Mech. Des. 143, 123401.

Ma, H.M., Gao, X.L., Reddy, J.N., 2008. A microstructure dependent Timoshenko beam model based on amodified couple stress theory. J. Mech. Phys. Solid. 56, 3379–3391.

Ma, X., Quan, W., Dong, Z., Dong, Y., Si, C., 2022. Dynamic response analysis of vehicle and asphalt pavement coupled system with the excitation of road surface unevenness. Applied. Math. Modelling. 104, 421–438.

Mahmood, S.S., Atiya, A.J., Abdulrazzak, F.H., Alkaim, A.F., Hussein, F.H., 2021. A Review on Applications of Carbon Nanotubes (CNTs) in Solar Cells. J. Med. Chem. Sci. 4, 225–229.

Mehralian, F., Beni, Y.T., 2018. Vibration analysis of size-dependent bimorph functionally graded piezoelectric cylindrical shell based on nonlocal strain gradient theory. J. Brazil. Society. Mech. Sci. Eng. 40. https://doi.org/10.1007/s40430-017-0938-y.

Miao, X., Li, C., Yulin, J., 2021. Free Vibration Analysis of Metal-Ceramic Matrix Composite Laminated Cylindrical Shell Reinforced by CNTs. Compos. Struct. 260, 113262.

Mohammad-Abadi, M., Daneshmehr, A.R., 2015. Modified couple stress theory applied to dynamic analysis of composite laminated beams by considering different beam theories. Int. J. Eng. Sci. 87, 83–102.

Mohammadimehr, M., Mohandes, M., 2015. The effect of modified couple stress theory on buckling and vibration analysis of functionally graded double-layer boron nitride piezoelectric plate based on CPT. J. Solid. Mech. 7, 281–298.

Mohammadimehr, M., Mohandes, M., Moradi, M., 2016. Size dependent effect on the buckling and vibration analysis of double-bonded nanocomposite piezoelectric plate reinforced by boron nitride nanotube based on modified couple. J. Vib. Control. 22, 1790–1807.

Mohammadimehr, M., Okhravi, S.V., Akhavan Alavi, S.M., 2018. Free vibration analysis of magneto-electro-elastic cylindrical composite panel reinforced by various distributions of CNTs with considering open and closed circuits boundary conditions based on FSDT. J. Vib. Control. 24, 1551–1569.

Mohandes, M., Ghasemi, A.R., 2016. Finite strain analysis of nonlinear vibrations of symmetric laminated composite Timoshenko beams using generalized differential quadrature method. J. Vib. Control. 22, 940–954.

Mohandes, M., Ghasemi, A.R., 2019. Discrepancies between free vibration of FML and composite cylindrical shells reinforced by CNTs. Mech. Adv. Compos. Struct. 6, 105–115.

Mohandes, M., Ghasemi, A.R., Irani-Rahagi, M., Torabi, K., Taheri-Behrooz, F., 2018. Development of beam modal function for free vibration analysis of FML circular cylindrical shells. J. Vib. Control. 24 (14), 3026–3035.

Mohandes, M., Ghasemi, A.R., 2019. A new approach to reinforce the fiber of nanocomposite reinforced by CNTs to analyze free vibration of hybrid laminated cylindrical shell using beam modal function method. Europ. J. Mech. 73, 224–234.

Moradi-Dastjerdi, R., Behdinan, K., 2021. Free vibration response of smart sandwich plates with porous CNT-reinforced and piezoelectric layers. Applied. Math. Modelling. 96, 66–79.

Mou, B., Bai, Y., 2018. Experimental investigation on shear behavior of steel beam-to-CFST column connections with irregular panel zone. Engin. Struct. 168, 487–504.

Nasution, M.K.M., Syah, R., Ramdan, D., Afshari, H., Amirabadi, H., Selim, M.M., Khan, A., Rahman, L., Sarjadi, M.S., Su, C.H., 2022. Modeling and computational simulation for supersonic flutter prediction of polymer/GNP/fiber laminated composite joined conical-conical shells. Arabian. J. Chemist. 15, 103460.

Ninh, D.G., Minh, V.T., Tuan, N.V., Hung, N.C., Phong, D.V., 2021. Novel Numerical Approach for Free Vibration of Nanocomposite Joined Conical–Cylindrical–Conical Shells. American Institute of Aeronautics and Astronautics. https://doi.org/10.2514/1.J059518.

Pan, S., Dai, Q., Safaei, B., Qin, Z., Chu, F., 2021. Damping characteristics of carbon nanotube reinforced epoxy nanocomposite beams. Thin-walled. Struct. 166, 108127.

Pashmforoush, F., 2020. Finite Element Analysis of Low Velocity Impact on Carbon Fibers/Carbon Nanotubes Reinforced Polymer Composites. J. Applied. Comput. Mech. 6, 383–393.

Qin, Z., Pang, X., Safaei, B., Chu, F., 2019. Free vibration analysis of rotating functionally graded CNT reinforced composite cylindrical shells with arbitrary boundary conditions. Compos. Struct. 220, 847–860.

Qin, Z., Shengnan, Z., Xuejia, P., Safaei, B., Chu, F., 2020. A unified solution for vibration analysis of laminated functionally graded shallow shells reinforced by graphene with general boundary conditions. Int. J. Mech. Sci. 170, 105341.

Reddy, J.N., 2004. Mechanics of Laminated Composite Plates and Shells. CRC Press.

Reddy, J.N., 2017. Energy Principles and Variational Methods in Applied Mechanics. JohnWiley, NewYork, NY.

Rezaiee-Pajand, M., Sobhani, E., Masoodi, A.R., 2020. Free vibration analysis of functionally graded hybrid matrix/fiber nanocomposite conical shells using multiscale method. Aerospace. Sci. Tech. 105, 105998.

SafarPour, H., Ghanbari, B., Ghadiri, M., 2019. Buckling and free vibration analysis of high speed rotating carbon nanotube reinforced cylindrical piezoelectric shell. Applied. Math. Modelling. 65, 428–442.

Shen, H.S., Xiang, Y., 2012. Nonlinear vibration of nanotube-reinforced composite cylindrical shells in thermal environments. Comput. Method. Applied. Mech. Eng. 213, 196–205.

Shen, H.S., Xiang, Y., Fan, Y., 2017. Nonlinear vibration of functionally graded graphene-reinforced composite laminated cylindrical shells in thermal environments. Compos. Struct. 182, 447–456.

Sheybani, M., Janghorban, M., Heidari, F., Taheri, K., 2021. Dynamics of nanocomposite plates. J. Brazilian. Society. Mech. Sci. Eng. 43, 335.

Shi, D.L., Huang, Y.Y., Hwang, K.C., Gao, H., 2004. The effect of nanotube waviness and agglomeration on the elastic property of carbon nanotube-reinforced composites. J. Eng. Mater. ASME. 126, 250–257.

Shokrieh, M., Rafiee, R., 2010. Prediction of mechanical properties of an embedded carbon nanotube in polymer matrix based on developing an equivalent long fiber. Mech. Res. Commun. 37, 235–240.

Sobhani, E., Masoodi, A.R., Ahmadi-Pari, A.R., 2021. Vibration of FG-CNT and FG-GNP sandwich composite coupled Conical-Cylindrical-Conical shell. Compos. Struct. 273, 114281.

Sobhani, E., Masoodi, A.R., 2021. Natural frequency responses of hybrid polymer/carbon fiber/FG-GNP nanocomposites paraboloidal and hyperboloidal shells based on multiscale approaches. Aerospace. Sci. Tech. 119, 107111.

Sobhani, E., Moradi-Dastjerdi, R., Behdinan, K., Masoodi, A.R., Ahmadi-Pari, A.R., 2022. Multifunctional trace of various reinforcements on vibrations of three-phase nanocomposite combined hemispherical-cylindrical shells. Compos. Struct. 279, 114798.

Sobhani, E., Masoodi, A.R., Civalek, O., Ahmadi-Pari, A.R., 2022. Agglomerated impact of CNT vs. GNP nanofillers on hybridization of polymer matrix for vibration of coupled hemispherical-conical-conical shells. Aerospace. Sci. Tech. 120, 107257.

Soleimani, I., Beni, Y.T., 2018. Vibration analysis of nanotubes based on two-node size dependent axisymmetric shell element. Archiv. Civil. Mech. Eng. 18, 1345–1358.

Syah, R., Ramdan, D., Elveny, M., Mohandes, M., Khan, A., Nouri, A., Albadarin, A.B., 2021. Computational simulation of critical speed and dynamic analysis of agglomerated CNTs/fiber/ polymer/ metal laminates rotating cylindrical shell. Arab. J. Chemist. 14, 103358.

Talebitooti, M., 2013. Three-dimensional free vibration analysis of rotating laminated conical shells: layerwise differential quadrature (LW-DQ) method. Arch. Appl. Mech. 83, 765–781.

Tao, C., Fu, Y., Dai, T., 2017. Dynamic analysis for cracked fiber-metal laminated beams carrying moving loads and its application for wavelet based crack detection. Compos. Struct. 159, 463–470.

Tornabene, F., Fantuzzi, N., Ubertini, F., Viola, E., 2015. Strong formulation finite element method based on differential quadrature: a survey. Appl. Mech. Rev. 67, 020801-1–55.

Tsai, S.W., Hoa, C.V., Gay, D., 2003. Composite materials, design and applications. CRC Press, Boca Raton.

Wang, C., Lai, J.C.S., 2000. Prediction of natural frequencies of finite length circular cylindrical shells. Appl. Acoust. 59, 385–400.

Wang, H., Zheng, X., Yuan, X., Wu, X., 2022. Low-Complexity Model-Predictive Control for a Nine-Phase Open-End Winding PMSM With Dead-Time Compensation. IEEE Trans. Power. Elec. 37, 8895–8908.

Yang, F., Chong, A.C.M., Lam, D.C.C., Tong, P., 2002. Couple stress based strain gradient theory for elasticity. Int. J. Solids. Struct. 39, 2731–2743.

Zeighampour, H., Beni, Y.T., 2014. Analysis of conical shells in the framework of coupled stresses theory. Int. J. Eng. Sci. 81, 107–122.

Zeighampour, H., Beni, Y.T., 2014. Cylindrical thin-shell model based on modified strain gradient theory. Int. J. Eng. Sci. 78, 27–47.

Zeighampour, H., Beni, Y.T., 2017. Size dependent analysis of wave propagation in functionally graded composite cylindrical microshell reinforced by carbon nanotube. Compos. Struct. 179, 124–131.

Zerrouki, R., Karas, A., Zidour, M., Bousahla, A.A., Tounsi, A., Bourada, F., Tounsi, A., Benrahou, K.H., Mahmoud, S.R., 2021. Effect of nonlinear FG-CNT distribution on mechanical properties of functionally graded nano-composite beam. Struct. Eng. Mech. 78, 117–124.

Zhang, C., Jin, Q., Song, Y., Wang, J., Sun, L., Liu, H., Dun, L., Tai, H., Yuan, X., Xiao, H., Zhu, L., Guo, S., 2021. Vibration analysis of a sandwich cylindrical shell in hygrothermal environment. Nanotechnology reviews (Berlin). 10, 414–430.

Zhang, X.M., Liu, G.R., Lam, K.Y., 2001. Vibration analysis of thin cylindrical shells using wave propagation approach. J. Sound. Vib. 239, 397–403.

Zhang, J., Zhao, Q., Ullah, S., Geng, L., Civalek, O., 2021. A new analytical solution of vibration response of orthotropic composite plates with two adjacent edges rotationally-restrained and the others free. Compos. Struct. 266, 113882.

Zhong, H., Yu, T., 2009. A weak form quadrature element method for plane elasticity problems. Appl. Math. Model. 33, 3801–3814.

Zhou, J., Bai, J., Liu, Y., 2022. Fabrication and Modeling of Matching System for Air-Coupled Transducer. Micromachines. 13, 781.

Zhu, P., Lei, Z.X., Liew, K.M., 2012. Static and free vibration analyses of carbon nanotube-reinforced composite plates using finite element method with first order shear deformation plate theory. Compos. Struct. 94, 1450–1460.